

HIGH PRESSURE SOLUBILITIES OF CARBON
DIOXIDE IN BENZENE, CYCLOHEXANE
NAPHTHALENE, AND TRANS-DECALIN

By

J. McRAY ANDERSON

Bachelor of Science

Oklahoma State University

Stillwater, Oklahoma

1983

Submitted to the Faculty of the Graduate College
of the Oklahoma State University
in partial fulfillment of the requirements for
the Degree of
MASTER OF SCIENCE
May, 1985

1

Thesis
1985
A547h
cop. 2



HIGH PRESSURE SOLUBILITIES OF CARBON
DIOXIDE IN BENZENE, CYCLOHEXANE,
NAPHTHALENE, AND TRANS-DECALIN

Thesis Approved:

Robert H. Robinson, Jr.

Thesis Adviser

B. L. Hynes

Mary L. Foutch

Norman N. Durham

Dean of the Graduate College

PREFACE

Isothermal solubilities of carbon dioxide in four solvents, benzene, cyclohexane, naphthalene, and trans-Decalin were measured at temperatures ranging from 40 to 150°C. An existing solubility apparatus was modified for the study of these binary mixtures. Other systems were also studied and are included in the thesis of Mr. Mark Barrick who worked jointly with me on this project. Interaction parameters in the Soave and Peng-Robinson equations of state were regressed from the solubility data and comparisons were made between the CO₂ solubilities in naphthenic and aromatic ring compounds. The significance of these results has been discussed.

I will be forever indebted to Professor Robert L. Robinson for his foresight, wisdom, and experience he so readily donated to this project. His devotion to teaching and his energy were the driving forces behind this work.

This study could never have been completed without the skilled craftsmanship of Mr. Heinz Hall, who created the stirred equilibrium cell which is the heart of the new apparatus. Mr. Hall deserves a special thanks for his patience and skills.

I would also like to thank and recognize Mr. Khaled Gasem for the sacrifices he made to explain and demonstrate the operation of the original apparatus. He has proved indispensable as a guide and mentor in the use of various software packages used throughout this work as well.

Special thanks are due Mr. Mark Barrick whose diligent labor as a coworker on this project has helped to create a superior solubility apparatus. His valuable drafting skills and many hours donated to this project are greatly appreciated. Ms. Kenda Morris also deserves thanks for the many hours she spent helping to prepare this thesis.

Finally, I would like to thank the Department of Energy (DE-FG22-83PC60039) for the financial support given this work.

TABLE OF CONTENTS

Chapter	Page
I. INTRODUCTION	1
II. LITERATURE REVIEW.	3
Previous Experimental Work.	3
Review of Equation of State Representation of CO ₂ + Hydrocarbon Systems.	4
III. THERMODYNAMIC PRINCIPLES OF VAPOR-LIQUID EQUILIBRIA.	8
IV. ANALYSIS OF ERRORS IN THE EXPERIMENTAL DATA.	16
V. EXPERIMENTAL APPARATUS AND OPERATING PROCEDURE	20
Experimental Apparatus.	21
General Description	21
Equilibrium Cell.	23
Rotating Magnet Assembly.	28
Storage Vessels	28
Pressure Measurements	30
Volumetric Injection Pumps.	31
Constant Temperature Baths.	31
Degassing Trap.	32
Fittings, Tubings, and Valves	34
Chemicals	34
Experimental Procedure.	35
Cleaning the Storage Cell	36
Cleaning the Equilibrium Cell	40
Charging and Degassing the Solvent.	41
Injecting the Solvent	43
Injecting the Solute Gas.	47
Measuring the Bubble Point.	50
Proper Determination of the Isothermal Solubility Curves.	55
Calibration of Pressure Transducers	57
VI. RESULTS AND DISCUSSION	60
Problems Encountered During Operation of Apparatus.	90

Chapter	Page
VII. CONCLUSIONS AND RECOMMENDATIONS.	92
Conclusions	92
Recommendations	93
REFERENCES.	94
APPENDIXES.	96
APPENDIX A - ERROR PROPAGATION FOR CO ₂ MOLE FRACTION	97
APPENDIX B - EXPLANATION OF THE PROGRAM USED TO CALCULATE PERCENTAGE UNCERTAINTY IN CO ₂ DENSITY100
APPENDIX C - COMPUTER PROGRAM USED TO CALCULATE CO ₂ DENSITY AS A FUNCTION OF TEMPERATURE AND PRESSURE.101
APPENDIX D - COMPUTER PROGRAM USED TO CALIBRATE PRESSURE TRANSDUCERS.108
APPENDIX E - EXPLANATION OF TABLE VI113

LIST OF TABLES

Table	Page
I. Preliminary Vapor Pressure Measurements	62
II. Solubility of CO ₂ in Benzene.	63
III. Solubility of CO ₂ in Trans-Decalin.	65
IV. Solubility of CO ₂ in Cyclohexane.	67
V. Solubility of CO ₂ in Naphthalene.	69
VI. Densities and Volumes Used to Calculate Solubilities for this Study.	71
VII. Soave and Peng-Robinson Equation of State Representations of CO ₂ Solubility Data.	79

LIST OF FIGURES

Figure	Page
1. Schematic Diagram of Bubble-Point Apparatus.	22
2. Overhead View of Bubble-Point Apparatus.	24
3. Stirred Equilibrium Cell	25
4. Cross Section of Stirring Mechanism.	27
5. Rotating Magnet Assembly	29
6. Degassing Trap	33
7. Schematic Diagram for Valve Identification	37
8. Injection Sheet.	44
9. Percentage Uncertainty in CO ₂ Density Versus Pressure.	48
10. P-V Data Sheet	52
11. Typical p_i Versus $(V_i - V_0)$ Plot	53
12. Typical p/x_{CO_2} Versus x_{CO_2} Plot.	56
13. Comparison of Measurements of CO ₂ Solubility in Benzene at 40°C	64
14. The Effect of Temperature on CO ₂ Solubility in Cyclohexane.	74
15. The Effect of Molecular Structure on CO ₂ Solubility in Six-Carbon Solvents.	75
16. The Effect of Molecular Structure on CO ₂ Solubility in Ten-Carbon Solvents	76
17. Soave Equation Representations of CO ₂ Solubilities in trans-Decalin and Cyclohexane.	78
18. Comparison of Data for CO ₂ Solubility in trans-Decalin at 75°C	81

Figure	Page
19. Comparison of Data for CO ₂ Solubility in Decalin at 50°C	82
20. Soave Equation Representation of CO ₂ Solubility in Naphthalene	83
21. Effect of Temperature on Interaction Parameters for CO ₂ + trans-Decalin.	85
22. Effect of Temperature on k_{ij} for CO ₂ + Cyclohexane	86
23. Effect of Temperature on l_{ij} for CO ₂ + Cyclohexane	87
24. Comparison of Solubility Data at one Atmosphere for CO ₂ + Cyclohexane.	89

CHAPTER I

INTRODUCTION

As more emphasis is placed on the conversion of coal to fluid fuels, a greater need arises for accurate methods to correctly predict the phase behavior of coal fluid mixtures. Although multicomponent multiphase fluids are present in all stages of coal conversion processes, models can be developed to represent the vapor-liquid equilibrium (VLE) of such systems based upon using data for binary mixtures composed of solvents and solutes representative of those compounds found in coal fluids (which contain higher concentrations of heavy naphthenic and aromatic compounds than petroleum fluids).

Development of good thermodynamic models requires accurate phase behavior data on the binary mixtures formed when specific solute gases are dissolved in heavy aromatic and naphthenic hydrocarbon solvents representative of those found in coal fluids. Because such data are extremely scarce, the major objective of this work was to modify an existing solubility apparatus and to produce solubility measurements for CO_2 in a series of aromatic and naphthenic solvents. The vapor-liquid phase behavior data were used to evaluate interaction parameters which are used in models to account for the unique behavior of each CO_2 + solvent binary mixture.

Specific systems studied in this work include two aromatic binary mixtures (CO_2 + benzene and CO_2 + naphthalene) and two naphthenic binary

mixtures (CO_2 + cyclohexane and CO_2 + trans-Decalin). Comparison of the behavior of CO_2 in these homomorphic naphthenic and aromatic ring compounds was done to delineate their effects on CO_2 solubility in coal fluids.

CHAPTER II

LITERATURE REVIEW

A literature search for information concerning the particular systems studied in this work (CO_2 + benzene, CO_2 + cyclohexane, CO_2 + naphthalene, CO_2 + trans-Decalin) was made to secure as much knowledge as possible about binary mixtures of CO_2 in both naphthenic and aromatic solvents. The results of this literature search are summarized in this chapter.

Previous Experimental Work

CO_2 + benzene binary mixtures have been studied by several authors (1, 2, 3, 4); however, no CO_2 + naphthalene data were found. Krichevskii and Sorina (5) investigated the CO_2 + cyclohexane system, but their work was at temperatures above those of this work. Low pressure solubilities of CO_2 + cyclohexane have been published by Dymond (6) and by Wilhelm and Battino (7), while Nagarajan, Chen, and Robinson (8) measured high pressure phase equilibria for the CO_2 + cyclohexane system at 160°F. Information on the CO_2 + trans-Decalin system is limited to a single article by Tiffin et al. (9).

Review of Equation of State Representation
of CO₂ + Hydrocarbon Systems

As a result of the interest in proper representations of the phase behavior of CO₂ + hydrocarbon mixtures, several models have been developed to accurately predict the phase behavior of such mixtures. This section includes a review of such models.

Graboski and Daubert (10), Mundis (11), and Huron et al. (12) have employed the Soave equation of state to model the behavior of CO₂ + hydrocarbon systems. Mixing rules which are variations of those described more specifically in Chapter III were used by all of the investigators; however, in each article, a single interaction parameter, k_{ij} , was used ($l_{ij} = 0.0$) to predict phase equilibrium.

Based on their results, Graboski and Daubert concluded that the search-optimization routine incorporated into the Soave equation to determine values of k_{ij} should be based on minimization of bubble point variance for best results (10); this is consistent with the choice of experimental technique used in the present work. In terms of bubble-point pressure (at a given T , x_j), their criterion for optimization was to minimize the value of σ^2 , as follows (10):

$$\sigma^2 = \sum_{i=1}^n [(p_i^{\text{calc}} - p_i^{\text{exp}})/p_i^{\text{exp}}]^2 \quad (1)$$

where n is the number of experimental data points measured for each isotherm, and $(p_i^{\text{exp}} - p_i^{\text{calc}})$ is the difference between the experimental and calculated saturation pressures for an experimental

point i . Using this criterion for optimization, these investigators computed interaction coefficients for CO_2 + hydrocarbon systems from data found in the available literature. They could not characterize the behavior of gas-aromatic and gas-naphthenic mixtures in a general fashion because the available literature binary data contained mostly gas-paraffin mixtures. Further, they concluded that, for many systems, the interaction coefficients are essentially independent of temperature and pressure (10).

In his study, also using the Soave equation, Huron found k_{ij} by searching for the minimum of the function Q at a given temperature and liquid composition (12).

$$Q = \sum_{i=1}^n [(y_i^{\text{calc}} - y_i^{\text{exp}})^2 + (p_i^{\text{calc}} - p_i^{\text{exp}})^2] \quad (2)$$

where $(y_i^{\text{exp}} - y_i^{\text{calc}})$ and $(p_i^{\text{exp}} - p_i^{\text{calc}})$ are the differences between the experimental and calculated vapor mole fractions and saturation pressures for an experimental point i and n is the number of experimental data points. No simple law or general correlation for the variation of k_{ij} with temperature for a given solvent was found by Huron and no correlation was found to relate k_{ij} to characteristic parameters of the hydrocarbons (number of carbon atoms, acentric factor, molecular weight, or critical constants). Huron went further to suggest that although no correlation was found, a relationship does exist between k_{ij} and solvent properties; however, he found no obvious means of predicting k_{ij} values from these solvent properties.

Mundis obtained data over a temperature range of -40 to 20°F which show the quantitative effects of naphthenic and aromatic solvents on the K-values of CO₂. The interaction parameters employed by Mundis are higher (but not significantly different) than those found by Huron or Graboski and Daubert. By necessity, Mundis evaluated his interaction parameters by direct fit of the Soave equation to the infinite dilution K value data measured in his study (11). Results of Mundis' comparison of naphthenic (cyclohexane) and aromatic (benzene) solvents show solubilities of CO₂ to be lower in naphthenic solvents than in aromatic solvents having the same number of carbon atoms.

The Peng-Robinson equation was used in a study by Lin (13). Mixing rules similar to those described more specifically in Chapter III were employed with $l_{ij} = 0.00$, as above. Solvents no heavier than n-decane were studied and interaction parameters were regressed by minimizing the unweighted deviation in vapor-liquid equilibrium ratios, K_i ,

$$\sum_{j=1}^n \sum_{i=1}^2 [(K^{\text{calc}} - K^{\text{exp}})/K^{\text{exp}}]_{ij}^2 \quad (3)$$

for both components for each isotherm studied and $K^{\text{calc}} - K^{\text{exp}}$ is the difference between the experimental and calculated vapor-liquid equilibrium ratios for experimental point j and component i . Lin's results indicate that there is no need to treat k_{ij} as temperature dependent in vapor-liquid equilibrium calculations for CO₂ + hydrocarbon mixtures. However, Lin does admit that best results are obtained by using the optimum value of k_{ij} for each specific CO₂ + hydrocarbon system at the temperature of interest (13).

In a study by Turek, et al. (14) on CO₂ + hydrocarbon systems, two interaction parameters were used to predict CO₂ + hydrocarbon mixture behavior with a modified form of the Redlich-Kwong equation of state described by Yarborough (15). The binary interaction parameters, k_{ij} and l_{ij} (expressed as functions of hydrocarbon acentric factor, ω_h) were determined simultaneously through numerical regression on binary VLE data. The objective function, F , used in that study was expressed in terms of the differences between the fugacity in the vapor phase, f_i^V , and the fugacity in the liquid phase, f_i^L deviations (14):

$$F = \sum_k \sum_{l=1}^{n_k} \sum_{i=1}^2 [f_i^V(T, p, y_i^{\text{exp}}) - f_i^L(T, p, x_i^{\text{exp}})]_{k,l}^2 \quad (4)$$

where index l refers to an individual VLE data point for binary system k , index i identifies an individual component within the binary, and n_k is the total number of points in system k . The authors reported that discrepancies among experimental data obscured the general trends of the parameters for the naphthenes and aromatics (14). (This emphasizes the importance of the present study.) Results of Turek's work show that use of two interaction parameters allows the equation of state to fit the data more accurately over a wider range of CO₂ solubilities.

CHAPTER III

THERMODYNAMIC PRINCIPLES OF VAPOR-LIQUID EQUILIBRIUM

A review of thermodynamic principles relevant to vapor-liquid equilibrium is presented in this section. The Soave and Peng-Robinson equations of state used to predict bubble-point pressures and solubilities are also described.

The fundamental criterion for phase equilibrium in a two-phase mixture of N components can be expressed in terms of temperature, T , pressure, p , and component chemical potentials, $\tilde{\mu}_i$, by the following equations (16):

$$T' = T'' \quad (5)$$

$$p' = p'' \quad (6)$$

$$\tilde{\mu}_i' = \tilde{\mu}_i'' \quad (i = 1, \dots, N) \quad (7)$$

where superscript ' indicates the vapor phase and superscript '' indicates the liquid phase. Thus, the relationship among temperature, pressure, and composition (through $\tilde{\mu}_i$) in a two-phase system at equilibrium is governed by the conditions that (17):

- a) The phases must be the same temperature and pressure, and
- b) The compositions of the phases must be such that, for each component, its chemical potential is the same in each phase.

If a model is employed relating the component chemical potentials to the phase compositions, temperature, and pressure, then the governing relations (expressed above) can be applied directly to the problem of calculation of equilibrium properties (dew points, bubble points, phase compositions) in terms of the variables listed ($T, p, \tilde{\mu}_i$). Unfortunately the chemical potential is not a convenient variable in practical applications, so it is normally replaced by a "better behaved" function, the fugacity, f_i . The chemical potential is related to the fugacity as follows.

For an ideal gas mixture at constant temperature, the value of the chemical potential for a specific component relative to its value in a pure state at pressure p^+ is

$$\tilde{\mu}_i - \mu_i^+ = RT \ln (py_i/p^+) \quad (8)$$

The simplicity of the form of Equation (8) can be retained for real mixtures by defining fugacity, f_i , which leads to the following relations for real gas mixtures:

$$\tilde{\mu}_i - \mu_i^+ = RT \ln (f_i/p^+) \quad (9)$$

and

$$\lim_{(p \rightarrow 0)} (f_i/py_i) = 1.0 \quad (10)$$

These equations are the definition of fugacity, f_i , and the reference pressure p^+ is one at which the gas behaves as an ideal gas. Writing

Equation (9) for both the vapor and liquid phases, respectively

$$\tilde{\mu}_i^v = \mu_i^+ + RT \ln (f_i^v / p^+) \quad (11)$$

$$\tilde{\mu}_i^l = \mu_i^+ + RT \ln (f_i^l / p^+) \quad (12)$$

and comparing to the original equilibrium criterion written as $\tilde{\mu}_i^v = \tilde{\mu}_i^l$, reveals that

$$f_i^v = f_i^l \quad (i = 1, \dots, N) \quad (13)$$

Substituting Equation (13) for Equation (7) enables the equilibrium criteria to be expressed in terms of fugacities rather than chemical potentials. The criteria of Equation (13) prove more convenient for practical applications.

Usually, the fugacity is not described directly, but rather in terms of its deviation from some idealized behavior. These deviations maybe expressed as fugacity coefficients and activity coefficients. The fugacity coefficient, ϕ_i , can be used to express deviations from ideal gas behavior:

$$\frac{f_i^v}{p y_i} = \phi_i^v \quad (14)$$

$$\frac{f_i^l}{p x_i} = \phi_i^l \quad (15)$$

Thus, by definition:

$$\lim_{(p \rightarrow 0)} \phi_i = 1.0 \quad (16)$$

Sometimes the activity coefficient, γ_i , is used in the liquid phase to express deviations from ideal liquid solution behavior ($f_i = f_i^0 x_i$):

$$\frac{f_i}{f_i^0 x_i} = \gamma_i \quad (17)$$

where f_i^0 is the fugacity of component i in the pure liquid state at the system temperature and pressure. In this work, emphasis is placed on determination of ϕ_i in both the liquid and vapor phases; γ_i is not used in phase equilibrium analysis for this study.

The fugacity coefficient, ϕ_i , must somehow be related to observable properties (eg. V , T , p , x_i), so that its value may be determined experimentally. Classical thermodynamics supplies the framework to develop the following integral which relates the fugacity coefficient, ϕ_i , to volumetric properties of the mixture:

$$\ln \phi_i = \frac{1}{RT} \int_V^\infty \left[\left(\frac{\partial p}{\partial n_i} \right)_{T,V,n_j} - \frac{RT}{V} \right] dV - \ln Z \quad (18)$$

where Z is the compressibility factor of the mixture, R is the universal gas constant, V is the volume, n_i is the moles of component i and n_j is the moles of component $j \neq i$. In Equation (18), all of the pVT behavior may be expressed in terms of the chosen equation of state, and the integral can be formally evaluated. The accuracy of the resultant ϕ_i

values then depends on how well the equation of state represents the mixture pVT behavior.

Several equation-of-state models are available to predict volumetric properties; however, two models, the Soave and Peng-Robinson equations of state, are most commonly used. Soave's modification of the Redlich-Kwong Equation (18) is presented as follows:

$$p = \frac{RT}{v - b} - \frac{a}{v(v + b)} \quad (19)$$

where

$$a = \sum_i \sum_j y_i y_j a_{ij} \quad (20)$$

$$b = \sum_i \sum_j y_i y_j b_{ij} \quad (21)$$

$$a_{ij} = (a_{ii} a_{jj})^{0.5} (1 - k_{ij}) \quad (22)$$

$$b_{ij} = \frac{1}{2} (b_{ii} + b_{jj}) (1 + l_{ij}) \quad (23)$$

$$a_{ii} = 0.4275 R^2 \frac{T_{ci} \alpha_i (T_{Ri})}{P_{ci}} \quad (24)$$

$$b_{ii} = 0.08664 RT_{ci}/P_{ci} \quad (25)$$

$$\alpha_i = [1 + m_i (1 - T_{Ri}^{0.5})]^2 \quad (26)$$

$$m_i = 0.480 + 1.574 \omega_i - 0.176 \omega_i^2 \quad (27)$$

where

R is the universal gas constant

T is the absolute temperature

T_c is the critical temperature

T_r is the reduced temperature

P_c is the critical pressure

v is the molar volume

ω is the acentric factor

a and b are constants

The empirical binary interaction parameters, k_{ij} and l_{ij} , are evaluated from experimental data. The Peng-Robinson Equation (19) is of the form

$$p = \frac{RT}{v - b} - \frac{a}{v(v + b) + b(v - b)} \quad (28)$$

where

$$a = \sum_i \sum_j y_i y_j a_{ij} \quad (29)$$

$$b = \sum_i \sum_j y_i y_j b_{ij} \quad (30)$$

$$a_{ij} = (a_{ii} a_{jj})^{0.5} (1 - k_{ij}) \quad (31)$$

$$b_{ij} = \frac{1}{2} (b_{ii} + b_{jj}) (1 + l_{ij}) \quad (32)$$

$$a_{ii} = 0.45724 \frac{R^2 T_{ci}^2 \alpha_i (T_{Ri})}{P_{ci}} \quad (33)$$

$$b_{ii} = 0.07780 \frac{RT_{ci}}{P_{ci}} \quad (34)$$

$$\alpha_i = [1 + \kappa(1 - T_{Ri}^{0.5})]^2 \quad (35)$$

$$\kappa = 0.37464 + 1.54226\omega - 0.26992\omega^2 \quad (36)$$

The mixing rules used for both the Soave and Peng-Robinson equations of state are identical to those presented by Turek, et al. (14).

Both the Soave and Peng-Robinson equations of state were employed in the present work. As suggested by Turek et al. (14), nonzero values for both k_{ij} and l_{ij} were used. The interaction parameters (k_{ij} , l_{ij}) were calculated by regressing the experimental binary solubility data to

minimize the objective function, S , which is the weighted sum of errors in predicted bubble-point pressures:

$$S = \sum_{i=1}^n \frac{(p_i^{\text{exp}} - p_i^{\text{calc}})^2}{\sigma_{ip}^2} \quad (37)$$

where

$$\sigma_{ip}^2 = (\sigma_{ip}')^2 + \left(\frac{\partial p}{\partial x_i}\right)^2 \sigma_{ix}^2 \quad (38)$$

σ_{ip}' is the uncertainty in the pressure gauge reading

x_i is the mole fraction of solute

σ_{ix} is the uncertainty of the mole fraction of solute

Further explanation of the data reduction techniques employed in this study is given by Gasem (4).

CHAPTER IV

ANALYSIS OF ERRORS IN THE EXPERIMENTAL DATA

When data are generated experimentally, errors are inherent in operation of the apparatus and measurements. These errors must be estimated to properly evaluate the acquired data. Both systematic and random errors contribute to "uncertainties" in the experimental results. Systematic errors stem from consistent deviations in observable measurements from their "true values". These deviations can usually be controlled by accurately calibrating and reading instruments used in operation. Random errors are less predictable in nature than systematic errors and are best evaluated using statistical analysis. Methods are discussed in this section to determine the effects of random errors inherent in the operation of the apparatus. Emphasis is placed on the cumulative effects these errors have on measurement of the bubble-point pressure.

Prime errors due to imprecisions in temperature, volume, and pressure measurements are established by repeated measurements and calibrations. In terms of standard deviations, these errors are estimated to be the following for the present apparatus:

$$\sigma_T = 0.05 \text{ K} \quad (39)$$

$$\sigma_V = 0.0025 \text{ cc} \quad (40)$$

$$\sigma_P = 0.05 \text{ psia} \quad (41)$$

The estimates for σ_V and σ_p are based on the ability to read the injection pump and pressure transducer, respectively; while σ_T is based on the ability of the temperature controller to hold the temperature at a given set point.

Uncertainties in calculated variables such as the liquid mole fraction, must be determined by error propagation. Appendix A demonstrates the error propagation for CO₂ liquid mole fraction which results in the following final equation:

$$\left(\frac{\sigma_{x_{CO_2}}}{x_{CO_2}}\right)^2 = x_s^2 \left[\left(\frac{\sigma_{\rho_{CO_2}}}{\rho_{CO_2}}\right)^2 + \left(\frac{\sigma_{V_{CO_2}}}{\sum V_{CO_2}}\right)^2 + \left(\frac{\sigma_{\rho_s}}{\rho_s}\right)^2 + \left(\frac{\sigma_{V_s}}{V_s}\right)^2 \right] \quad (42)$$

where:

- $\sigma_{x_{CO_2}}$ is the uncertainty in CO₂ liquid mole fraction
- x_{CO_2} is the measured CO₂ liquid mole fraction
- x_s is the measured solvent liquid mole fraction (1 - x_{CO_2})
- $\sigma_{\rho_{CO_2}}$ is the uncertainty in CO₂ gas density
- ρ_{CO_2} is the CO₂ gas density
- $\sigma_{V_{CO_2}}$ is the uncertainty in reading the CO₂ gas injection pump
- $\sum_{i=1}^n V_{CO_2}$ is the total volume of CO₂ gas injected into the equilibrium cell in n total injections
- σ_{ρ_s} is the uncertainty in solvent density
- ρ_s is the solvent density

σ_{V_s} is the uncertainty in reading the solvent injection pump
 V_s is the volume of solvent injected

Estimated fractional uncertainties ($\frac{\sigma}{\rho}$) in the CO₂ gas density and solvent densities are 0.0015 and 0.001, respectively. The fractional uncertainty in CO₂ density is the sum of the uncertainty due to temperature and pressure variations (approximately 0.0005, see Appendix B) and the uncertainty associated with the IUPAC equation used to calculate the CO₂ density (0.001, see Figure 13 of Reference 23) while the fractional uncertainty in the solvent densities is typical of uncertainties for liquid densities found in literature sources. After substituting the values above and the data for a typical injection (Table VI, naphthalene at 150°C injection 1), Equation (42) reduces to:

$$\sigma_{x_{CO_2}} = 0.0016 x_1 x_2 \quad (43)$$

which results in a maximum estimated error in CO₂ liquid mole fraction measurement of $\sigma_{x_{CO_2}} = 0.0004$. As indicated in Chapter VI, some of the isotherms studied show errors in measured solubilities which are close to the value calculated here; however, a value of 0.001 for the actual error in CO₂ liquid mole fraction is indicated from the data. This suggests that the method of injection leaves room for error which is not taken into consideration with Equation (42).

Uncertainties in dependent variables such as bubble-point pressure, σ_{BPP} , are also determined through error propagation. These

uncertainties in bubble-point pressure measurement are due to both prime and propagated errors and can be expressed by the following Equation

(4):

$$\sigma_{\text{BPP}}^2 = \sigma_p^2 + \left(\frac{\partial P}{\partial X_{\text{CO}_2}}\right)_T^2 \sigma_{X_{\text{CO}_2}}^2 + \left(\frac{\partial P}{\partial T}\right)_X^2 \sigma_T^2 \quad (44)$$

Assuming the temperature contribution term is negligible in Equation (44),

$$\sigma_{\text{BPP}} = [(0.05)^2 + \left(\frac{\partial P}{\partial X_{\text{CO}_2}}\right)^2 (0.0004)^2]^{0.5} \quad (45)$$

which results in an estimated error in bubble-point pressure ranging from 0.5 psia (CO₂ + benzene 40°C) to 2.3 psia (CO₂ + naphthalene 150°C).

CHAPTER V

EXPERIMENTAL APPARATUS AND OPERATING PROCEDURES

Many experimental apparatus and operating procedures have been used to study vapor-liquid equilibrium. In most cases investigators use variations of one of the three following methods:

- a) Phase compositions are measured as a function of pressure at a constant temperature
- b) Phase compositions are measured as a function of temperature at constant pressure
- c) The pressures and/or temperatures where condensation or boiling occurs are measured at constant composition

Experimental apparatus which encompass each of the above mentioned methods are currently in use (20, 21, 22). Of special interest to this study are those investigators who developed their apparatus to incorporate the bubble-point approach (method c above) to vapor-liquid equilibrium data acquisition. Sage et al. (22) developed such an apparatus, and the method employed in this study is similar to theirs with added design details for handling solvents which are solid at room temperature and a new method of agitating the binary mixture. Tiffin et al. (9) have also developed a similar apparatus; however they use a method other than the bubble-point approach to acquire data.

The bubble-point approach to VLE data acquisition was chosen for this study for several reasons. The bubble-point method is simple and

precise and does not require use of analytical instruments (such as chromatographs) for phase analysis. It is efficient and produces data which are quite adequate for present purposes and very reliable. Details of the bubble-point method and the apparatus used in this study are discussed in the following sections. Because the apparatus and procedure were the same as those used for the acquisition of Mr. Mark Barrick's (26) data, the following sections are identical in both theses.

Experimental Apparatus

The apparatus used in this study was designed for measurement of isothermal bubble-point pressures of liquid mixtures. Of particular interest were measurements on solute gases in solvent liquids which would solidify at room temperature. The apparatus was originally designed and operated by Gasem (4), but it was extensively redesigned and reconstructed for the present study. The modifications increased the rate of data collection and eliminated effects of room temperature fluctuations on the measured pressures. A schematic diagram of the apparatus is shown in Figure 1 and a description is given below.

General Description

The operation of the apparatus, to measure bubble-point pressures of binary mixtures, involves combining known amounts of solute gas and solvent liquid in an equilibrium cell. The mixture, maintained at constant temperature, is stirred and compressed so that the solute gas is forced into solution in the solvent. The bubble-point pressure for the given mixture is taken as the pressure at which the vapor phase

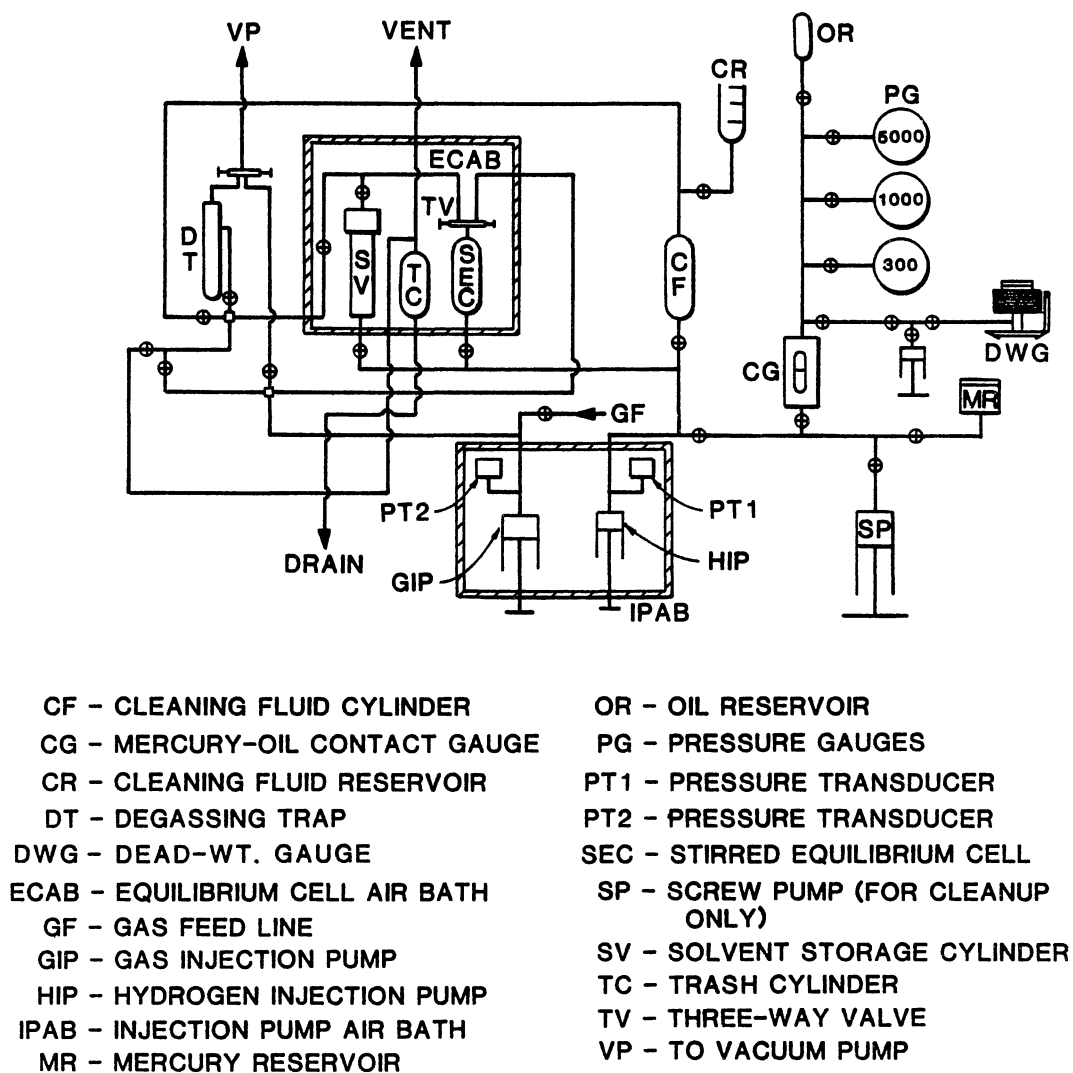


Figure 1. Schematic Diagram of Bubble-Point Apparatus

disappears. A general description of the arrangement of the apparatus follows.

The bubble-point apparatus is supported on two adjacent tables (see Figure 2). The larger table holds the equilibrium cell air bath (ECAB, abbreviations refer to nomenclature of Figures 1 and 2) and the control panel, with the equilibrium cell air bath temperature controller on a lower shelf. Upon the smaller table is the injection pump air bath (IPAB). A lower shelf was built into the smaller table to house the cleaning pump (CP) and the injection pump air bath temperature controller.

The control panel supports much of the apparatus, including the valves, tubing, magnet drive motor controller, pressure gauges, and digital pressure and temperature indicators. The degassing trap (DT), cleaning fluid storage cell (CF), and cleaning fluid reservoir (CFR) are also mounted on the control panel.

Equilibrium Cell

The central component of the apparatus is a variable volume stirred equilibrium cell. This equilibrium cell is a 304 stainless steel tubular reactor (High Pressure Equipment Company Incorporated, catalog number TOC-6), modified to become the stirred equilibrium cell (SEC) shown in Figure 3.

The first modification of the reactor was to machine the top 2.25 inches of the reactor from an outside diameter of 1.50 inches to 1 inch. This was done to increase the magnetic coupling between the drive magnets (DM) and stirrer magnets (SM). Next, the bottom port of the top plug was tapped to allow attachment of a stirrer support pin (SSP).

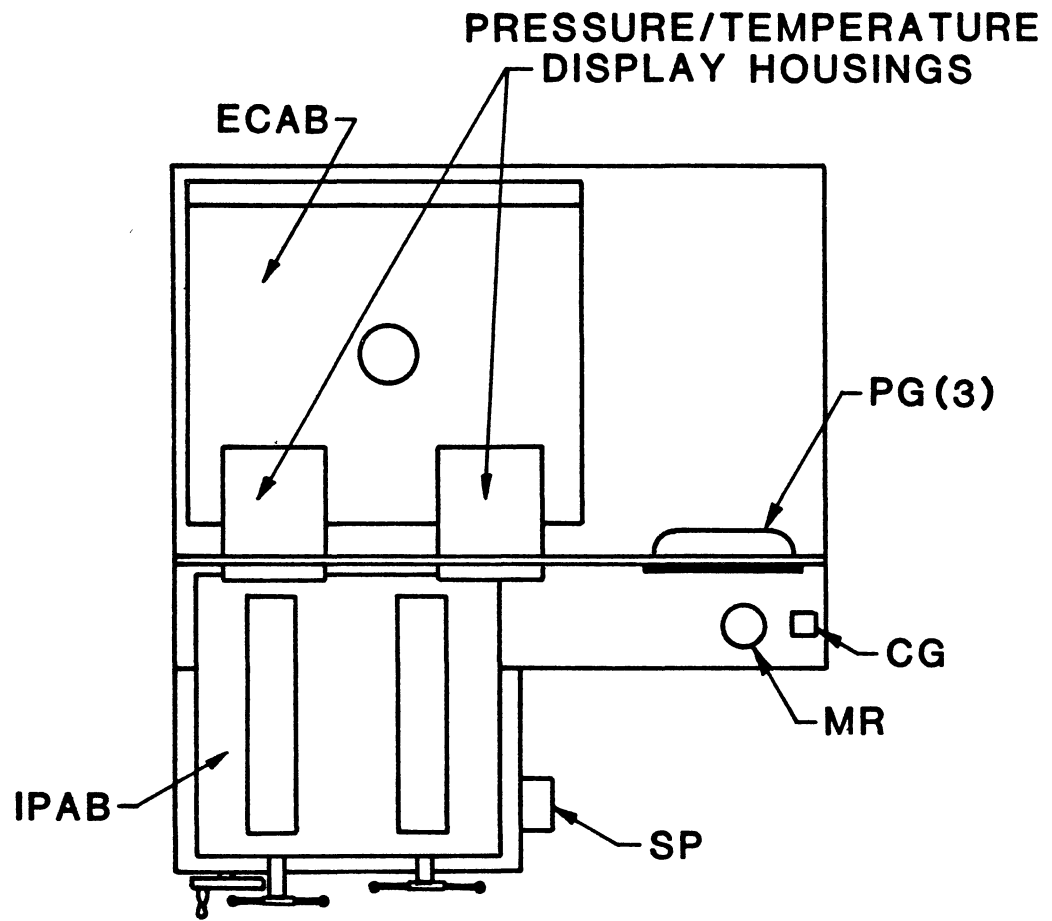
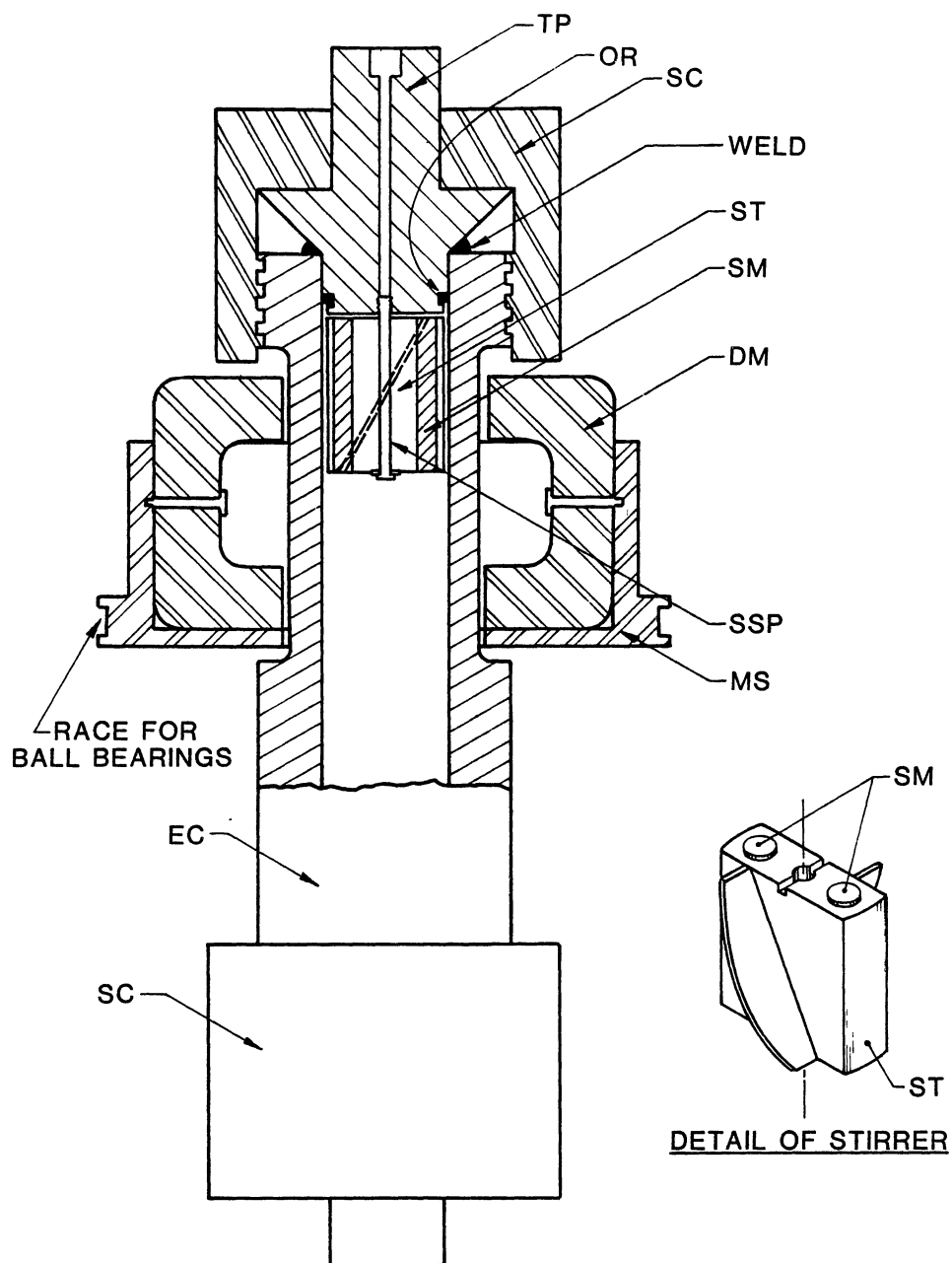


Figure 2. Overhead View of Bubble-Point Apparatus



- DM - DRIVE MAGNETS
 EC - EQUILIBRIUM CELL (CYLINDRICAL)
 MS - ROTATING MAGNET SUPPORT
 OR - O RING
 SC - SCREW CAP
 SM - STIRRER MAGNETS
 SSP - STIRRER SUPPORT PIN
 ST - STIRRER
 TP - TOP PLUG

Figure 3. Stirred Equilibrium Cell

After modification of the cell, a persistent high pressure leak from the "O" ring seal on the top plug (TP) was discovered. To eliminate this leak, the top plug was beveled downward (to avoid trapping chemicals) and welded to the body of the equilibrium cell.

The stirrer, machined from cylindrical aluminum stock, is 1" long and has a rectangular body with an impeller blade on each side (see detail, Figure 3). Two cylindrical stirrer magnets were mounted in the stirrer symmetrically about and parallel to the stirrer vertical exit. The stirrer is attached to the base of the top plug by the stirrer support pin (SSP).

A flow channel for introduction or removal of chemicals from the top of the equilibrium cell was made by drilling a hole down the center of the stirrer support pin for the length of its threads. A second hole was then drilled horizontally across the threads, intersecting the first hole (see Figure 4). The threads were then filed flat on planes perpendicular to the horizontal hole. In addition, the stirrer was slotted across the top. Acting together, these modifications allowed easy chemical access to the inside of the equilibrium cell for injecting or cleaning purposes.

The equilibrium cell has an internal volume of approximately 37 cc. The effective volume of the cell can be varied by introduction or withdrawal of mercury (which acts as a fluid piston) through the bottom of the cell. Chemical injections to the cell were made at the top of the cell through a short section of small diameter stainless steel tubing connected to a stainless steel three way valve (High Pressure Equipment Company Incorporated, catalog number 15-15 AF1). Separate

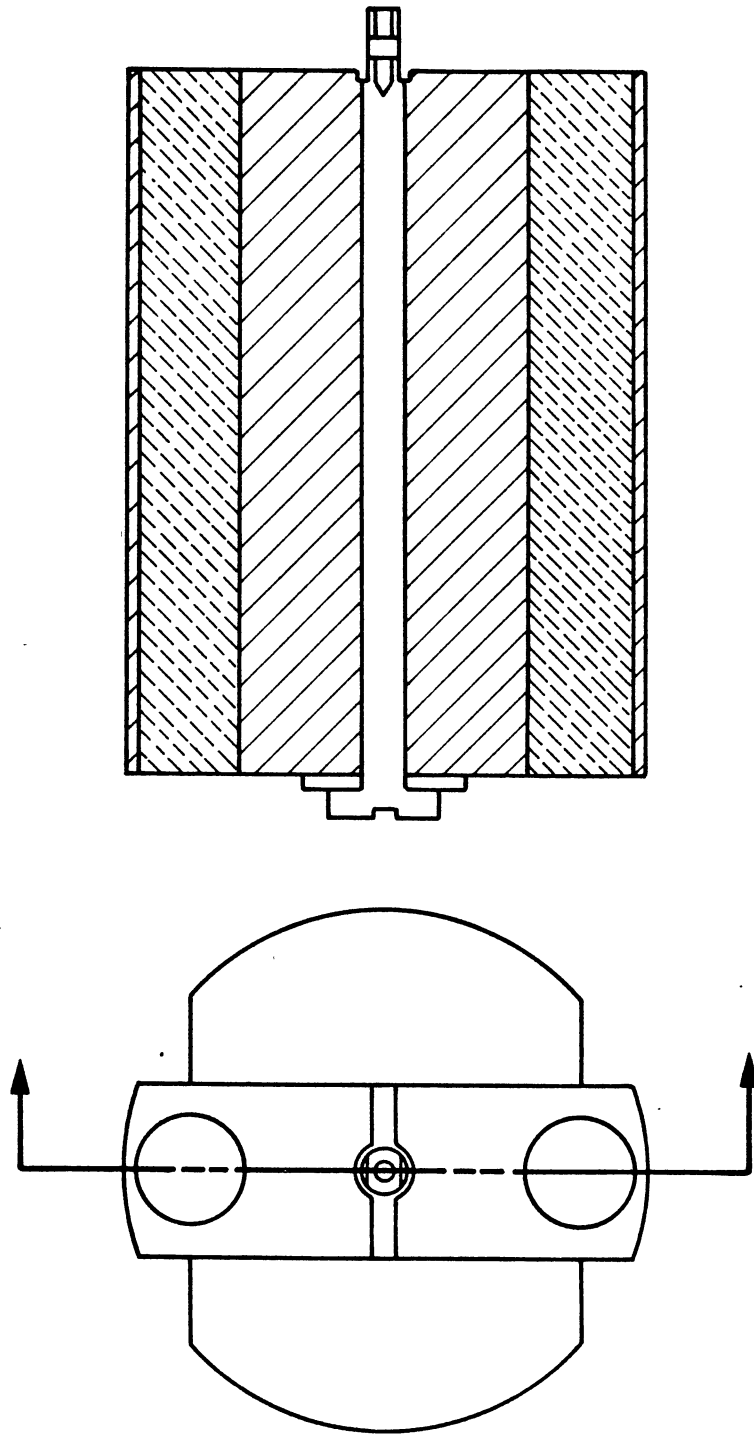


Figure 4. Cross Section of Stirring Mechanism

inlet lines for the solute gas and solvent liquid were connected to this valve, which controlled chemical access to the cell.

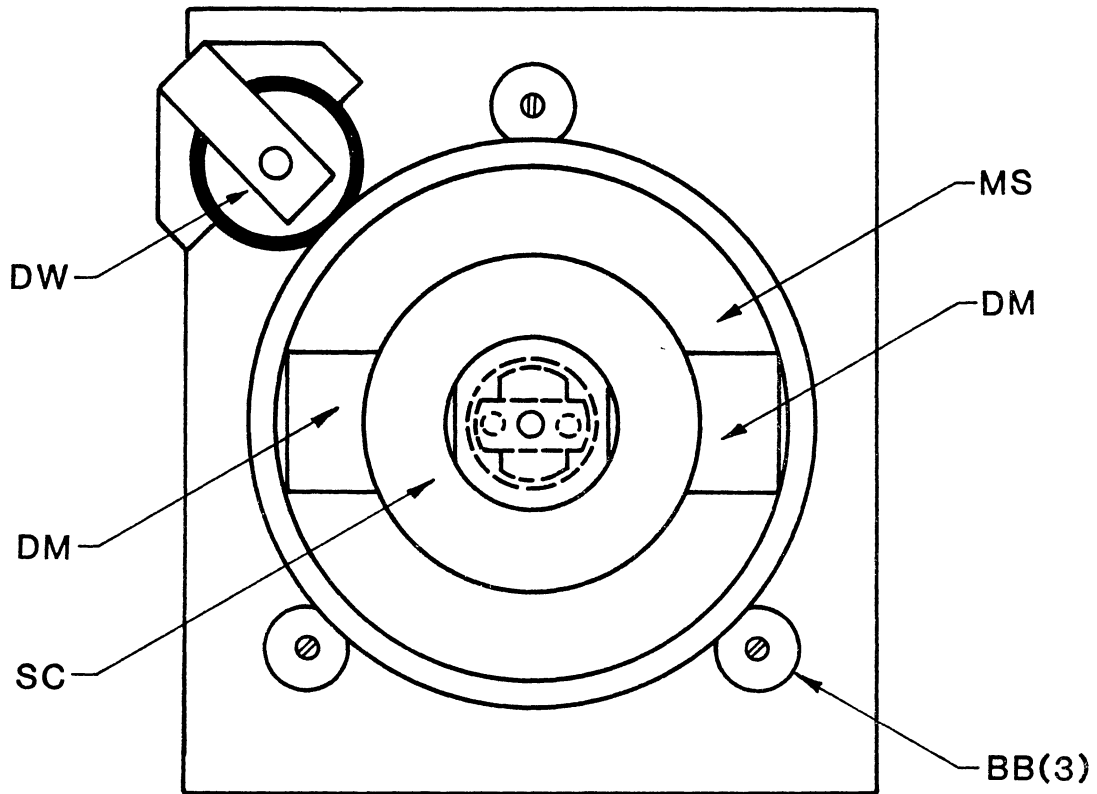
Rotating Magnet Assembly

A rotating magnet assembly was used to drive the stirrer within the equilibrium cell. Figure 5 shows a top view of this assembly.

Three ball bearings (BB) (Fafnir, catalog number S5KDD) held the rotating magnet support (MS) in place while allowing it to spin freely. The rotating magnet support is doughnut shaped and was fabricated in two sections so it can be opened to allow removal of the equilibrium cell from the air bath. The two drive magnets (DM) are bolted, opposite each other, to the walls of the rotating magnet support. A 1/50 horsepower variable speed motor (Bodine Electric Company, model series 200, type NSH-12) is used to power the drive wheel (DW), which contacts the edge of the rotating magnet support. The motor is mounted on top of the equilibrium cell air bath and is connected to the drive wheel by a variable-length drive shaft. A motor speed controller (Bodine Electric Company, model 901, type BSH-200) was used to maintain the rotating magnet support speed of 124 revolutions per minute.

Storage Vessels

Several cylinders were employed for either injection or storage purposes (see Figure 1). The solvent storage cylinder (SV) is a high-pressure reactor bomb with a screw type closure (High Pressure Equipment Company Incorporated, catalog number OC-3). It is housed inside the equilibrium cell air bath so that heavy solvents (solids at room



BB - BALL BEARINGS
DM - DRIVE MAGNETS
DW - DRIVE WHEEL
MS - ROTATING MAGNET SUPPORT
SC - SCREW CAP

Figure 5. Rotating Magnet Assembly

temperature but liquids at operating temperature) can be melted and degassed prior to their use. The solute gas is stored in a 25 cc gas injection pump (GIP). The injection pump (Temco Incorporated, model 25-1-10-HAT), kept at constant temperature within the injection pump air bath, facilitates direct injection of the solute gas to the equilibrium cell.

The cleaning fluid cylinder (CF), a 250 cc high pressure stainless steel cylinder, is used to store cleaning fluid for injection to the equilibrium cell or solvent storage cylinder during clean up before or after experimental runs. A 150 cc glass buret was used as a reservoir (CR) for charging cleaning fluid to the cleaning fluid storage cylinder. Solvent and cleaning fluid could be displaced from the solvent storage cylinder or cleaning fluid storage cylinder, respectively, by injecting a volume of mercury into the bottom of these cylinders, which displaces an equal volume of their contents.

The trash cylinder (TC), a 250 cc stainless steel cylinder, is housed within the equilibrium cell air bath and used to receive liquids being expelled from the apparatus during clean up.

A 250 cc mercury reservoir (MR) was used to maintain an adequate volume of mercury within the system.

Pressure Measurements

Equilibrium cell, solvent injection, and solute injection pressures were measured with pressure transducers (Sensotec Incorporated, model STJE 1890) with a range of 0-3000 psi. These pressure transducers were kept at constant temperature in the injection pump air bath. Pressures

are displayed on digital readouts (Sensotec Incorporated, model 450D) with a resolution of 0.1 psi.

Pressures within the equilibrium cell, solvent storage cylinder, and cleaning fluid cylinder are transmitted directly to the solvent transducer (PT1) through mercury-filled lines. The pressure of the solute gas is measured directly by the solute transducer (PT2). At the beginning of the study of each binary mixture, the hydrocarbon pressure transducer was calibrated against a dead weight tester (Ruska Instrument Corporation, model number 2400.1).

Volumetric Injection Pumps

Three precision positive displacement pumps were used to operate the apparatus. A 10 cc pump (Temco Incorporated, model 10-1-12 H) was used for injecting solvent and for varying the effective volume of the equilibrium cell during data collection. This pump has a pressure rating of 10,000 psi and a resolution of 0.005 cc. Solute injections were made with a 25 cc pump (Temco Incorporated, model 25-1-10-HAT) which has a pressure rating of 10,000 psi and a resolution of 0.005 cc. Both pumps were maintained at constant temperature in the injection pump air bath.

To clean the apparatus, a 500 cc pump (Ruska Instrument Corporation, model 2210-801) was used. This pump is rated at 12,000 psi and has a resolution of 0.02 cc.

Constant Temperature Baths

Two air baths were used to maintain constant temperatures for components of the apparatus used for injection and pressure measuring

purposes. The equilibrium cell air bath (ECAB) (Hotpack, model 200001) houses the equilibrium cell, solvent storage cylinder, and trash cylinder. Temperature of this oven is maintained within 0.1°C by a Halikainen proportional-integral controller, model 1053 A, which was used to replace the original temperature control system on the air bath.

The injection pumps and pressure transducers are housed in the injection pump air bath. This air bath was fabricated from $1/2$ " plywood and lined with fiberglass insulation. A Halikainen proportional-integral controller, model 1053 A, is also used to maintain the temperature in this air bath within 0.1°C of the setpoint, which was 50.0°C throughout this study.

The temperatures of both air baths are measured with precisions of 0.1°C using separate platinum resistance thermometers connected to identical digital readouts (Fluke Incorporated, model 2180 A) which have a resolution of 0.01°C . Periodic ice point measurements confirmed the claimed accuracy of 0.1°C .

Degassing Trap

Prior to bubble-point measurements, the solvent liquid must be degassed to remove air or any volatile contaminants in the solvent storage cylinder.

The degassing trap is a 100 cc, 1" diameter glass tube with a ground glass connection and a glass top which accommodates inlet and outlet lines (see Figure 6). To degass the solvent, the solvent storage cylinder is evacuated. If any of the solvent vaporizes during degassing, it is carried along and condensed at the bottom of the degassing trap, ahead of the vacuum pump. Once degassing of the solvent

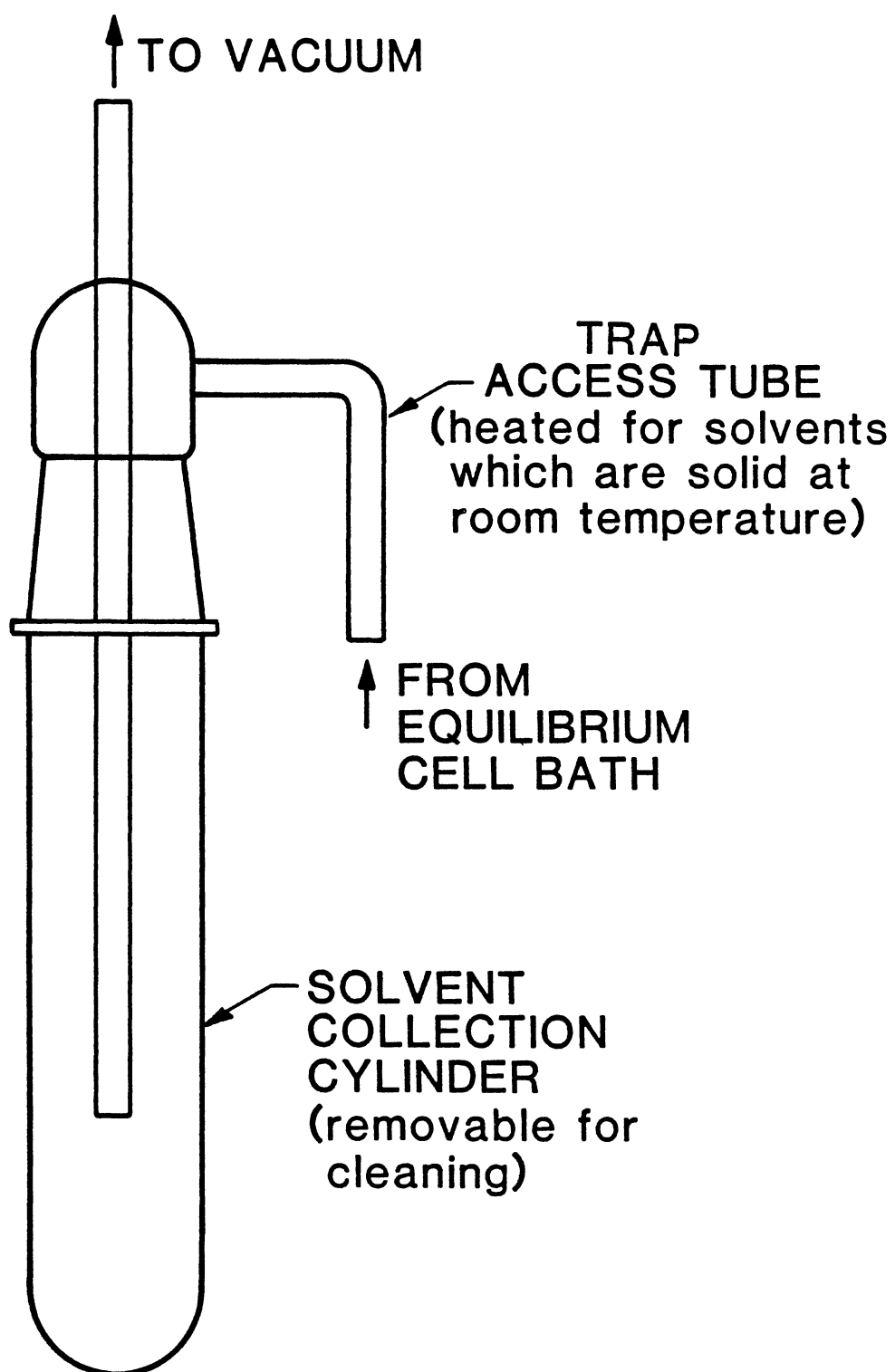


Figure 6. Degassing Trap

has been completed, the bottom tube of the trap is removed and emptied.

The lines between the solvent storage cylinder and degassing trap were wrapped with heating tape to prevent solvent solidification in the lines. A variac was used to control the temperature of the heating tapes.

Fittings, Tubing, and Valves

All fittings, tubing, and valves (High Pressure Equipment Company) used in construction of this apparatus were made of 316 stainless steel and rated at 15,000 psi. One-sixteenth inch tubing and valves were used for pressure measurement lines to minimize dead volumes where necessary. One-eighth inch tubing and valves were used throughout the rest of the apparatus.

Chemicals

All materials used in this study were obtained from commercial suppliers and no further purification was attempted. The suppliers and stated purities of the chemical are as follows:

<u>Chemicals</u>	<u>Source</u>	<u>Stated Purity (mol %)</u>
Carbon Dioxide	Union Carbide Company	99.99
n-Pentane	Fisher Scientific Company	Spectro Grade
Benzene	Aldrich Chemical Company	Reagent Grade
Naphthalene	Aldrich Chemical Company	99+
trans-Decalin	Aldrich Chemical Company	99+
Cyclohexane	Phillips Petroleum Company	99+

Experimental Procedure

This section contains a step-by-step procedure for properly measuring solubilities using the apparatus described in the previous section. Two steps in the operation of the apparatus are extremely critical in obtaining accurate data: injection of the solvent/solute and measurement of the pressure which determines the solubility (bubble-point pressure). Special care must be taken during the injections to assure accurate measurement of the amount of each component injected into the equilibrium cell so that the composition of the mixture in the cell will be evaluated correctly. Caution and patience must also be exercised when measuring the bubble-point pressure; some mixtures require up to two hours to reach a stable pressure after they have been disturbed. Methods are suggested herein for detecting if an isotherm of data is possibly in error. These simple yet reliable methods are included as a check against errors made in either of the two critical steps mentioned above.

Throughout this chapter, the terms solubility and bubble-point pressure are used interchangeably. Because different terminologies exist in thermodynamic literature, the terms solubility and bubble point are both used to describe a single phase binary mixture at the point where the gas phase has just dissolved totally into the liquid phase. Thus, the data taken in this work may be viewed as the solubility of the gas (mole fraction) in the liquid at given temperature and pressure or as the bubble-point pressure of the mixture at given temperature and composition.

in 1.4p
introduction

Cleaning The Storage Cell

Before the solvent storage vessel (SV, Figure 1) can be used to store a hydrocarbon solvent, it must be properly cleaned of the previous contents so that the new solvent is not contaminated. The cleaning procedure is as follows:

1. If the storage vessel contains solvents which are solid at room temperature, turn on the heating tape and allow the disposal lines outside the equilibrium cell air bath (ECAB) to come to a temperature above the melting point of the solvent. Open valves V1, V6, V10, and OV1 (for location of all valve abbreviations, refer to Figure 7). Using the cleaning pump (CP), purge any solvent from the solvent storage vessel by pumping mercury into the bottom of the storage vessel until mercury can be seen in the sight tube (ST) located just down-line from the trash cylinder (TC). The sight tube is viewed through a window in the equilibrium cell air bath so that the bath can remain closed and at constant temperature during cleanup.

2. Open V2 and purge the sight tube with solute gas (typically the solute gas is kept at approximately 200 psia for purge purposes). Close V1 and V2 once the mercury and solvent in the sight tube have been blown into the trash cylinder. If the solute gas does not displace the mercury and solvent from the sight tube, a plug may have formed somewhere in the trash lines. Heat any exposed trash lines directly with a heat gun until the solute gas has cleared the plug from the lines and purged the sight tube of any mercury or solvent left from the storage vessel.

3. Withdraw mercury from the bottom of the solvent storage vessel to create a 70 to 80 cc space in the storage vessel. By opening V2, a

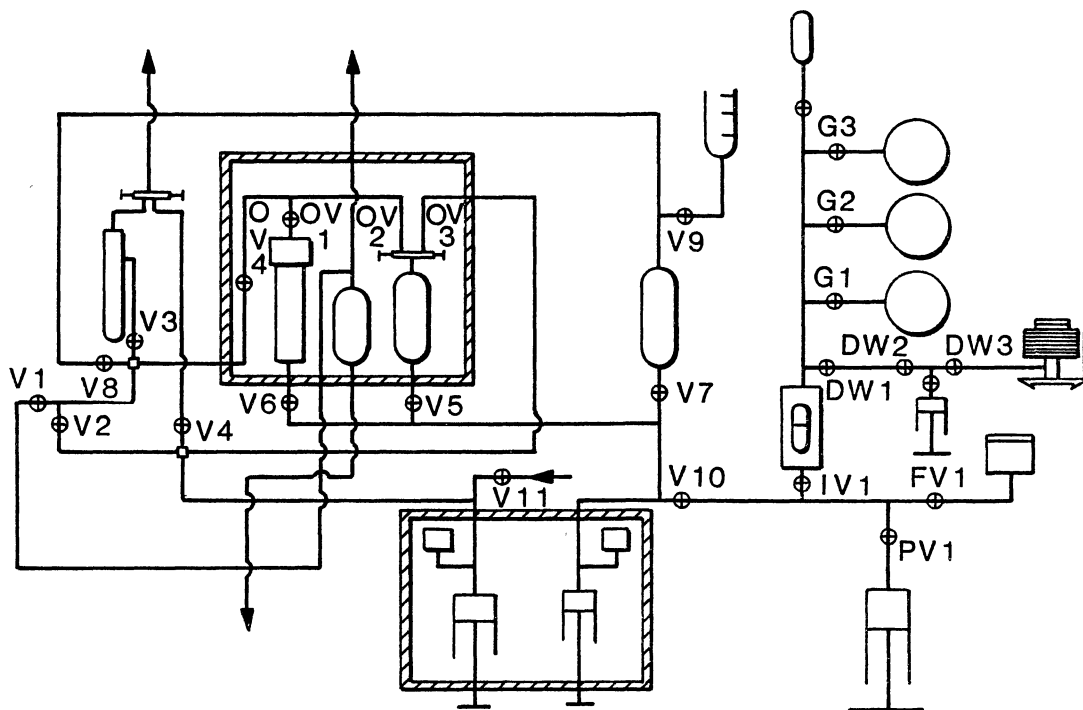


Figure 7. Schematic Diagram for Valve Identification

pressure head may be established above the mercury in the storage vessel to aid in the removal of mercury from the cell. Solute gas used for a pressure head must be vented through V1 after the mercury has been removed from the vessel.

4. Close V1 and V6, open V7 and V9, and inject mercury into the cleaning fluid storage cylinder (CF) using the cleaning pump until mercury can be seen in the bottom of the cleaning fluid reservoir (CR). Fill the reservoir with approximately 100 cc of cleaning fluid (normally n-pentane or benzene) by pouring the fluid into the opening at the top of the reservoir. Draw the cleaning fluid into the cleaning fluid storage cylinder by withdrawing 80 to 90 cc of mercury back into the cleaning pump, then close V9.

5. Pressurize the cleaning fluid to assure it is totally liquid by pumping mercury from the cleaning pump into the cleaning fluid storage cylinder until a pressure reading higher than the vapor pressure of the cleaning fluid is indicated on the hydrocarbon transducer readout. Open V8 and inject cleaning fluid into the storage vessel by use of the cleaning pump. Continue until the storage cell is full of cleaning fluid. Close V7 and V8, open V6 and increase the pressure in the storage vessel to a level which assures that the cleaning fluid in the vessel is all liquid. Allow the cleaning fluid to remain in the solvent storage vessel for a period of time (15 to 20 minutes) so that any remaining solvent in the storage vessel will dissolve in the cleaning fluid.

6. Repeat steps 1 through 5 twice to clean the cell a total of three times. After the charge of cleaning fluid has been removed following steps 1 and 2 and 80 to 90 cc of space have been left in the

storage vessel as explained in step 3, remove any residual cleaning fluid vapors from the vessel by turning on the vacuum pump, allowing it to create a sufficient vacuum, and then opening valves VV1, V3, and OV1.

A sufficient vacuum is indicated when the vacuum gauge reads 500 millitorr or less. A "perfect" vacuum would register zero millitorr on the vacuum gauge; however, the current vacuum system is capable of producing a vacuum of only 200 millitorr under the best possible circumstances (ie. clean trash trap, tight seals on all connections, clean oil in vacuum pump, vacuum pump working properly). During most evacuations of the storage vessel the vacuum gauge registers 500 millitorr. This measure of vacuum has proved sufficient in all cleanings of the storage vessel; however, allowing the vacuum to register above 500 millitorr should be avoided because this will not assure proper evacuation of the storage vessel.

Because the hydrocarbon transducer was set at 0.0 psia under vacuum conditions, the pressure reading from the hydrocarbon transducer should fall immediately and approach 0.0 psia after OV1 has been opened. The transducer will indicate a small pressure reading (2.0 to 3.0 psia) as long as vapors from the cleaning fluid remain in the storage vessel; however, the pressure reading should fall slowly to 0.0 psia as the cleaning fluid vapors are evacuated from the storage cell. If the pressure in the storage vessel does not fall immediately after OV1 has been opened, a plug has formed somewhere in the vacuum lines. To remedy this problem apply direct heat with the heat gun to any exposed areas of the lines until the pressure falls as expected.

Cleaning the Equilibrium Cell

To measure correct solubilities, the equilibrium cell must be properly cleansed of any foreign material prior to beginning a run. The following procedure will create a clean cell ready for injection of solute and solvent.

1. If the solvent being removed from the equilibrium cell is solid at room temperature, turn on the heating tape and allow it to come to temperature above the melting point of the solvent. Close valve OV1, V3, VV1, and V6 and open valves V1, V5, and OV2. Using the cleaning pump, displace any mixture from a previous experiment out of the equilibrium cell (SEC) by injecting mercury into the bottom of the equilibrium cell until mercury can be seen in the sight tube.

2. Open V2 and purge the sight tube with solute gas (watch for plugs and remove as described earlier). Close V1 and V2 after the sight tube is clear.

3. Remove mercury from the cell to create a 20 cc space in the equilibrium cell. By opening V2, solute gas pressure may be established above the mercury in the equilibrium cell to aid in removal of mercury from the cell. This solute gas must be vented through V1 after the mercury has been removed from the cell.

4. Close V1 and V5, open V7 and V9, and inject mercury into the cleaning fluid storage cylinder (using the cleaning pump) until mercury can be seen in the bottom of the cleaning fluid reservoir. Fill the cleaning fluid reservoir with 70 to 80 cc of cleaning fluid. Draw cleaning fluid into the storage cylinder by withdrawing 70 to 80 cc of mercury back into the cleaning pump then close V9 and V7.

5. Open V7 and pressurize the cleaning fluid to assure it is completely liquid. Open V8 and inject cleaning fluid into the equilibrium cell by use of the cleaning pump. Continue until the equilibrium cell is full of cleaning fluid. Close V7, V8, and OV2, open V5 and pressurize the equilibrium cell to a level which assures that the cleaning fluid remains liquid in the cell. Turn on the stirrer to assist the cleaning fluid in dissolving any remaining solvent. Allow the cleaning fluid to remain in the equilibrium cell for 10 to 15 minutes before removing it.

6. Repeat steps one through five twice omitting step four each time. Step four is omitted the second and third time because enough cleaning fluid has been placed in the cleaning fluid storage cylinder initially to complete all three subsequent cleaning fluid injections. After the third charge of cleaning fluid has been removed and a 20 cc space created in the equilibrium cell, switch on the vacuum pump. Open VV1 and V3 after the vacuum gauge indicates the vacuum pump is creating a sufficient vacuum (as explained in step six of solvent storage vessel cleaning procedure). Open OV2 and allow the equilibrium cell to be evacuated for six to seven hours to assure all cleaning fluid vapors and foreign matter are evacuated from the cell. The hydrocarbon pressure transducer reading should fall immediately after OV2 is opened; approaching zero as the cleaning fluid vapors are removed from the equilibrium cell.

Charging and Degassing the Solvent

1. After being properly cleaned and evacuated, the solvent storage vessel is ready to be charged with solvent. To charge the storage

vessel, unscrew the cap from the top of the vessel and carefully remove the plug by pulling straight up (to avoid scratching the sealing surface of the storage vessel). Examine the empty storage vessel by holding a mirror over the top opening of the vessel and adjusting the mirror so that the inside of the vessel can be viewed. If the vessel walls and mercury in the vessel both appear clean, fill the vessel with hydrocarbon solvent. Should residue be observed on the vessel walls or on the mercury at the bottom of the vessel, then the vessel should be swabbed with a soft cloth or rag dipped in cleaning fluid, always being careful not to scratch the sealing surface of the storage vessel. Solid hydrocarbons should be tightly packed into the solvent storage vessel so that a maximum amount of hydrocarbon can be placed in the cell (a space of 20 to 30 cc must be left above the hydrocarbon solvent in the storage vessel to allow room for replacement of the plug). To complete the charging procedure carefully replace the plug and screw down the cap of the storage vessel.

2. After properly charging the storage vessel, turn on the vacuum pump and allow it to create a sufficient vacuum. If a solid hydrocarbon has been placed in the storage vessel, the heating tape must be turned on to supply heat to all of the exposed lines used in degassing, thus preventing a solid plug of solvent from forming in these lines. Before proceeding, the heating system should run for fifteen minutes to allow the lines to reach a temperature above the melting point of the solvent.

3. Open VV1, V3, and OV1 to allow any dissolved air to be removed from the solvent in the storage vessel. The transducer reading should fall immediately after OV1 has been opened, approaching zero as air is removed from the storage vessel. If the pressure in the vessel does not

drop, a plug has probably formed in the degassing lines and must be removed by direct heating from the heat gun.

4. Allow the hydrocarbon solvent to degas for approximately four hours while checking periodically for traces of solvent in the degassing trap (DT). Any solvent collected in the degassing trap can not be used for injection, so it is important to keep the amount of solvent lost to the degassing trap to a minimum. Volatile hydrocarbon solvents must be watched closely because they evaporate readily under vacuum and much of the solvent can be lost to the degassing trap. When valve OV1 is opened, air is pulled into the degassing trap, normally carrying traces of solvent with it as it bubbles up the trap access tube (Figure 6) into the trap. As more air is evacuated from the storage vessel, the bubbling is reduced and eventually subsides (normally after approximately four hours; less time for volatile solvents). When the solvent can not be seen bubbling up the trap access tube, the degassing is complete. Close OV1, V3, and VV1 to isolate the solvent from the vacuum lines and turn off the vacuum pump. Pump mercury from the cleaning pump into the storage vessel to move solvent into the evacuated space left in the storage vessel and injection lines after degassing. Vent the pump by breaking the connections from the pump to the light condensable trap located in the hood.

Injecting the Solvent

So that a complete record of the injection can be kept for future reference, an injection sheet (Figure 8) is used to record all necessary information. The sheet is prepared by recording the date and the name, density, and molecular weight of the solvent in their designated

INJECTION SHEET

Date: _____

SOLVENT INJECTION

Solvent Name: _____

Time_i: _____P_i: _____Temp Pump
Bath : _____x_i: _____Temp Cell
Bath : _____x_f: _____Time_f: _____P_f: _____ $\Delta V = (\text{_____}) (\text{_____}) = \text{_____}$ Solvent $\rho = \text{_____}$ M. Wt. = _____
() $\Delta n \text{ solvent} = \text{_____}$

n solvent = _____

SOLUTE INJECTION

Solute Name: _____

Time_i: _____P_i: _____Temp Pump
Bath : _____x_i: _____Temp
Room : _____x_f: _____Time_f: _____P_f: _____ $\Delta V: \text{_____}$ Solute $\rho = \text{_____}$ M. Wt. = _____
() $\Delta n \text{ solute} = \text{_____}$ n total: _____

n solute = _____ x solute: _____

OBSERVATIONS: _____

Figure 8. Injection Sheet

places. Once the sheet is prepared, the solvent is injected as described below.

1. When the desired temperatures have been set and both air baths allowed to come to temperature (normally requiring four to five hours for all metal parts in the ovens to reach thermal equilibrium), record the temperatures on the injection sheet, then open V5 and OV1. After the evacuated lines leading to the equilibrium cell from the storage vessel have been completely filled with solvent, compress the solvent to a level above the solvent vapor pressure. Once the solvent has been compressed, close V10 and monitor the pressure in the storage vessel until it becomes constant. In practice, approximately one hour is required to reach a constant pressure in the storage vessel.

2. When the storage vessel pressure becomes constant, record the pressure reading on the injection sheet. Note the initial volume reading on the hydrocarbon injection pump (HIP) and record this value on the sheet also. After recording the volume, open OV2 and advance the injection pump until approximately 7cc (for CO₂ solubility studies) of solvent have been injected into the equilibrium cell. To finish the injection, close OV2 and adjust the hydrocarbon injection pump until the pressure in the storage vessel returns to the original value recorded before OV2 was opened. After reestablishing the original pressure reading, record the final volume reading from the injection pump.

3. By subtracting the initial volume reading from the final volume reading of the injection pump, the volume of mercury injected is calculated. This value must be adjusted slightly to determine the amount of solvent injected to the equilibrium cell since the mercury density changes as it moves from one air bath temperature to the

other. The adjustment factor is calculated by dividing the density of mercury at the temperature of the cell bath (ECAB) into the density of mercury at the temperature of the pump bath (IPB). The moles of solvent injected are then calculated from the following equation:

$$n_{\text{HC}} = \left[\rho_{\text{HC}} (V_2 - V_1) \frac{\rho_{\text{Hg}}(T_{\text{pb}})}{\rho_{\text{Hg}}(T_{\text{cb}})} \right] / \text{MW}_{\text{HC}} \quad (46)$$

where

- n_{HC} is the moles of hydrocarbon solvent injected, gmol
- ρ_{HC} is the density of the hydrocarbon solvent, gm/cc
- V_2 is the final volume reading of the injection pump, cc
- V_1 is the initial volume reading of the injection pump, cc
- $\rho_{\text{Hg}}(T_{\text{pb}})$ is the density of mercury at the temperature of the pump bath, gm/cc
- $\rho_{\text{Hg}}(T_{\text{cb}})$ is the density of mercury at the temperature of the cell bath, gm/cc
- MW_{HC} is the molecular weight of the solvent

4. After calculating the moles of solvent injected, close V6, open V10, and return the injection pump to the original volume read before the injection. As the injection pump is drawn back, fill the void left in the injection pump with mercury from the cleaning pump. When the injection pump has been returned to its original position, open V5 to monitor the pressure in the equilibrium cell. The pressure in the equilibrium cell should be equal to the vapor pressure of the injected solvent. If the vapor pressure of the injected solvent is less than

atmospheric pressure, more mercury should be injected into the equilibrium cell until the pressure in the cell is above atmospheric pressure so that no air can enter the equilibrium cell from a possible leak under vacuum.

Injecting the Solute Gas

1. Once the amount of solvent injected into the equilibrium cell has been calculated, a desired mole fraction of solute is chosen at which to measure the first mixture bubble-point pressure. The mole fraction chosen depends on the nature of the solvent and the desired range of solubilities to be measured. Using the chosen mole fraction and the moles of solvent injected, an estimate of the moles of solute gas to be injected is calculated from the following equation:

$$n_{SG} = \frac{n_{HC} x_{SGi}}{(1.0 - x_{SGi})} \quad (47)$$

where

n_{SG} = estimated moles of solute gas to be injected

n_{HC} = moles of solvent injected

x_{SGi} = chosen initial mole fraction of solute gas

2. Set the solute gas injection pump (GIP) initial reading to 0.000 cc and allow the pressure in the injection pump to stabilize at some pressure between 600 and 900 psia. This pressure range is chosen because the solute gas densities used in this work are relatively insensitive to T, p variations within this range (Figure 9). (Appendix B explains how Figure 9 was developed). Record this pressure on the

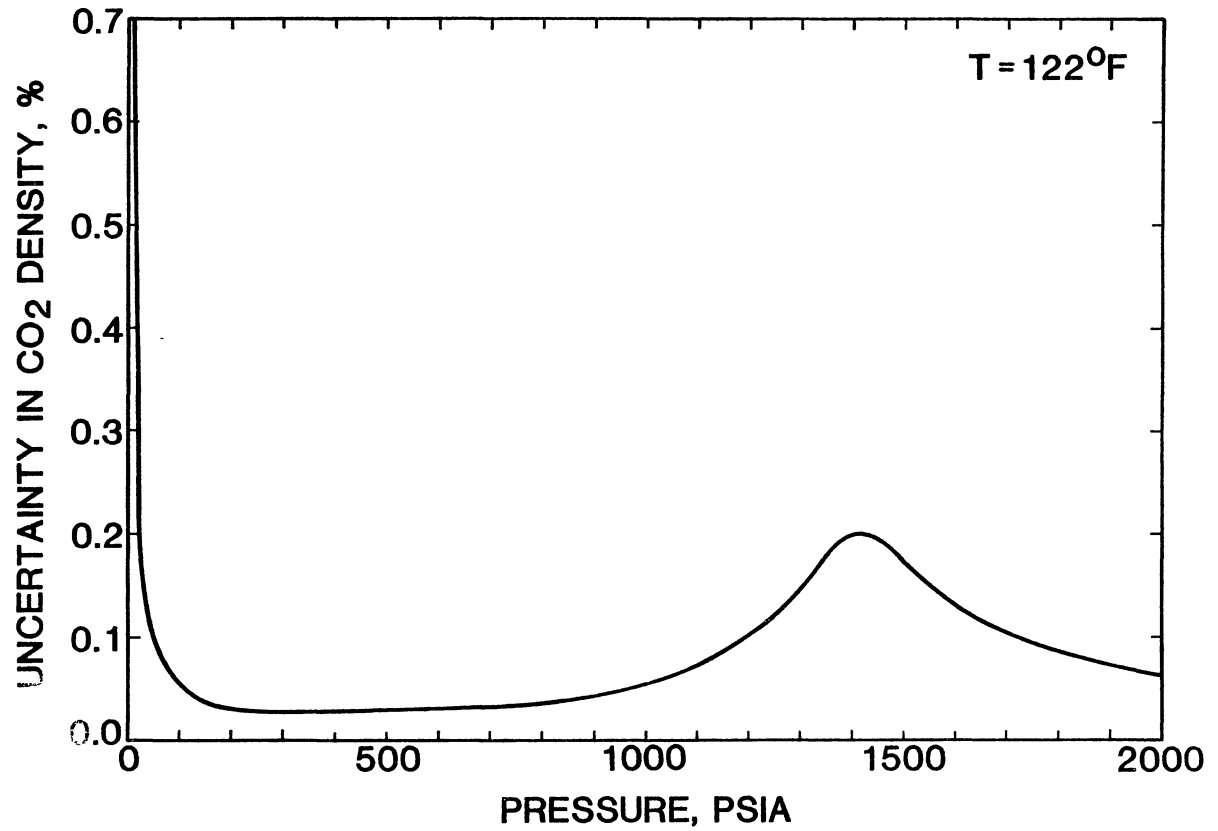


Figure 9. Percentage Uncertainty in CO₂ Density Versus Pressure

injection sheet. At the recorded pressure and temperature of the pump bath, calculate the solute gas density. A program was developed for calculating density of carbon dioxide as a function of temperature and pressure (Appendix C) using equations published by IUPAC (23). This program provides an accurate and efficient means of calculating CO₂ gas phase densities.

3. Record the solute gas density on the injection sheet and use the following equation to calculate an estimate of the volume of solute gas to be injected.

$$V_{SG} = n_{SG} MW_{SG} / \rho_{SG} (T_{GIP}, P_{GIP}) \quad (48)$$

where

V_{SG} = estimated volume of solute gas to be injected

n_{SG} = estimated moles of solute gas to be injected
calculated from Equation (45)

MW_{SG} = Molecular weight of the solute gas

$\rho_{SG} (T_{GIP}, P_{GIP})$ = Density of solute gas evaluated at the
temperature and pressure of the solute gas
injection pump

Advance the piston in the solute injection pump by the amount calculated in Equation (48). Carefully and slowly open OV3 and allow the pressure in the solute injection pump to return to approximately the original pressure reading recorded on the injection sheet. Quickly close OV3, then adjust the solute injection pump until the exact original pressure reading is reestablished in the pump. After allowing sufficient time for the pressure in the solute injection pump to reach the original

value (normally requires 2 to 3 minutes to stabilize at recorded pressure), note the volume reading on the pump and record this value on the injection sheet. Calculate the actual moles of solute gas injected from the tabulated density, the solute molecular weight, and the final volume read from the injection pump. When the actual moles of solute injected are known, the actual mole fraction of solute can be calculated by the following relation and the injection is complete.

$$x_{SG} = \frac{n_{SG}}{n_{SG} + n_{HC}} \quad (49)$$

where

x_{SG} = actual mole fraction of solute gas

n_{SG} = moles of solute gas injected into the equilibrium cell

n_{HC} = moles of hydrocarbon solvent injected into the equilibrium cell

Measuring the Bubble Point

1. Usually after injection of the solvent and solute, the vapor-liquid interface is about 10 cc below the top of the equilibrium cell. The gas phase must be totally collapsed for the bubble-point pressure to be determined. To accomplish this, open V10 and V5, and turn on the stirrer. Use the cleaning pump to introduce mercury into the equilibrium cell until the gas phase is forced into solution, being careful not to exceed the 2,000 psia limit on the pressure transducer.

2. Allow the pressure to stabilize at a level approximately 200 psi above the expected bubble-point pressure of the mixture. This will assure the solute is completely dissolved in the solvent and a single-

phase fluid exists in the equilibrium cell. Isolate the cleaning pump from the apparatus by closing V10.

3. When the pressure stabilizes, note the volume reading on the solvent injection pump. A p-V data sheet (Figure 10) is used to record all data points taken during the bubble point measuring procedure. Record on this sheet the volume from the pump, the temperature of both air baths, and the corresponding stabilized pressure read from the hydrocarbon transducer.

4. Rotate the solvent pump handle counter-clockwise 0.01 cc removing that volume of mercury from the equilibrium cell. Record the new volume reading from the pump on the p-V data sheet. Allow the pressure to stabilize, exercising patience to assure the proper (stabilized) pressure is tabulated. Record the pressure on the data sheet.

5. Repeat step four three times. Plot the data recorded on the p-V data sheet as p_i vs $(V_i - V_0)$, where p_i and V_i represent the system pressure and volume of point i , respectively, and V_0 represents the original volume reading on the p-V data sheet. Figure 11 shows results for a typical p-V traverse. The steep slope of the single phase line indicates an all-liquid composition in the equilibrium cell because liquids are relatively incompressible and the pressures are greatly effected by small changes in volume. Fit the best line possible through the four data points and extrapolate the line down to a pressure level below the expected bubble-point pressure.

6. Rotate the pump handle counter-clockwise again, but only remove 0.005 cc of mercury from the equilibrium cell (smaller increments in volume are used nearer the bubble-point pressure to more accurately

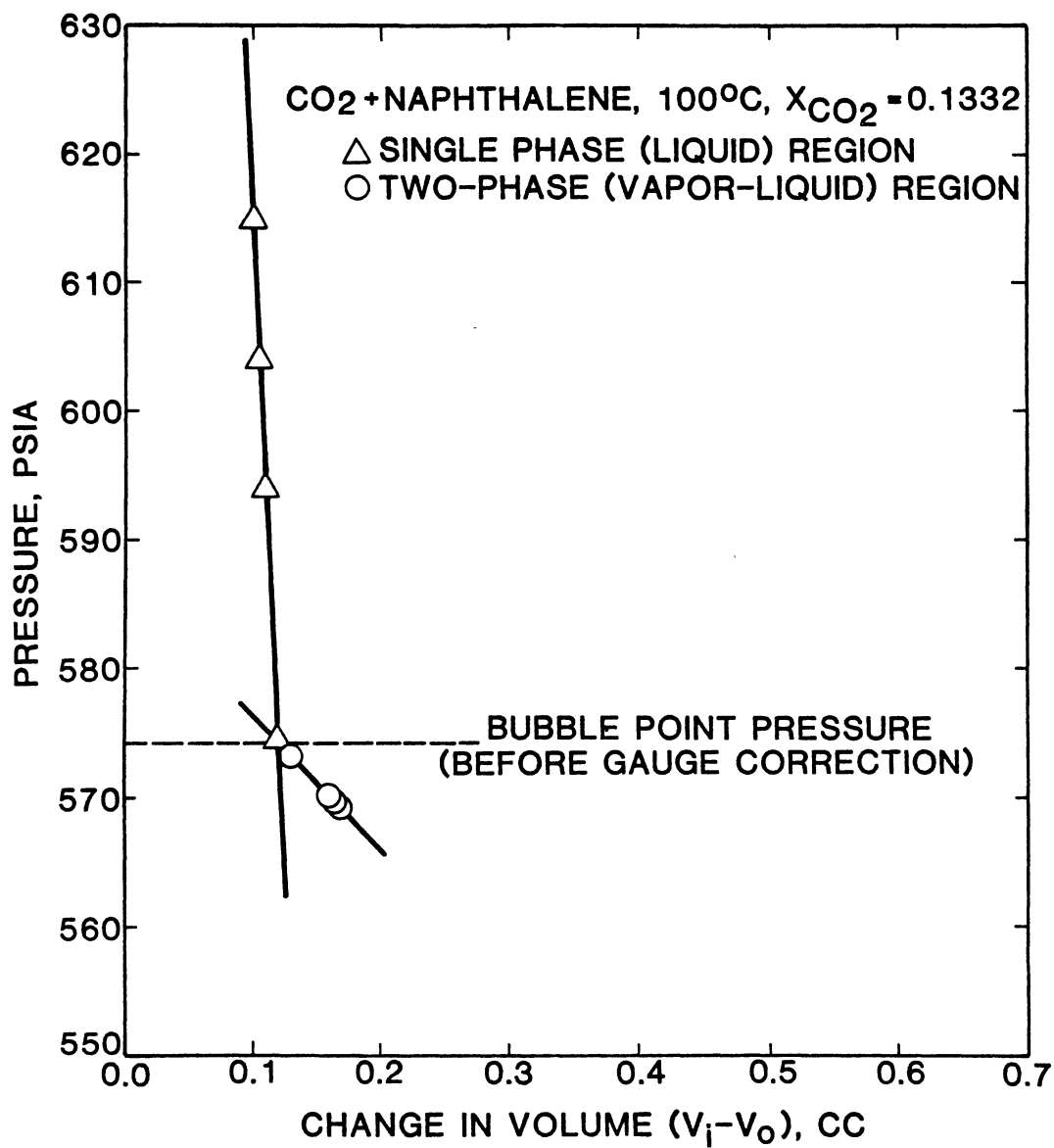


Figure 11. Typical p_i Versus $(V_i - V_0)$ Plot

determine the correct pressure). After the pressure stabilizes, record it and the volume reading from the solvent injection pump on the p-V data sheet. Plot this point as before and check to see if it lies on the extrapolated single phase line. If the point is on the line, the fluid in the equilibrium cell is still single-phase liquid.

7. Repeat step six until the measured pressure deviates from the extrapolated single-phase line when it is plotted on the p_i vs $(V_i - V_0)$ graph (this p will lie above the line). Such a behavior indicates that the fluid in the equilibrium cell has separated into vapor and liquid phases.

8. Withdraw 0.005 cc from the equilibrium cell, again recording the volume reading from the solvent pump and the corresponding pressure after it has stabilized.

9. Plot the resulting data point and repeat step eight until enough points have been plotted (as described in step five) to establish a two-phase line (three or four points are usually sufficient).

10. Extrapolate the two-phase line to intersect the single-phase line. As indicated in Figure 11, the intersection of the two lines determines the bubble-point pressure of the composition under study.

11. From the transducer calibration record find two transducer pressure readings which bound the experimentally measured bubble point. A typical transducer calibration record is shown in Appendix D (see HYDROCARBON TRANSDUCER CORRECTIONS, Appendix D computer output). Linearly interpolate between the two boundary values to find the transducer gauge correction which corresponds to the measured bubble point. Adjust the measured bubble point by the corresponding gauge correction and the measurement is complete.

Proper Determination of the Isothermal Solubility Curves

Because no visible observation of the cell contents is possible to check the exact amount of material charged to the cell, other methods must be used to determine experimentally whether the solubilities measured are acceptable. A useful method is described below.

To properly establish an experimental pressure-composition isotherm, a system combining the bubble-point pressure measurements from two separate hydrocarbon solvent injections is used. First solvent is injected following the proper procedure. Solute gas is then injected and bubble-point pressures measured at three or four mole fractions of solute gas. After the final pressure has been measured, the equilibrium cell is cleaned and a second solvent injection is made at the same temperature. Additional solute injections are made with the second solvent injection and their respective pressures are measured.

The relation between the mole fraction of solute, x , and the bubble-point pressure, p , can be conveniently observed by plotting the seven experimental values as p/x vs x . The points should lie on a smooth curve as demonstrated in Figure 12. If the points from the separate solvent injections do not lie on single smooth curve, then at least one of the two runs is in error, and another solvent injection must be made to determine which of the injections is incorrect.

The above mentioned method is a convenient means of determining erroneous solubilities because the p/x values magnify any inherent pressure errors by the reciprocal of the mole fraction. The magnified error is easily identified on the graph as a point which does not lie on the smooth curve created by the correct measurements. Also, by matching

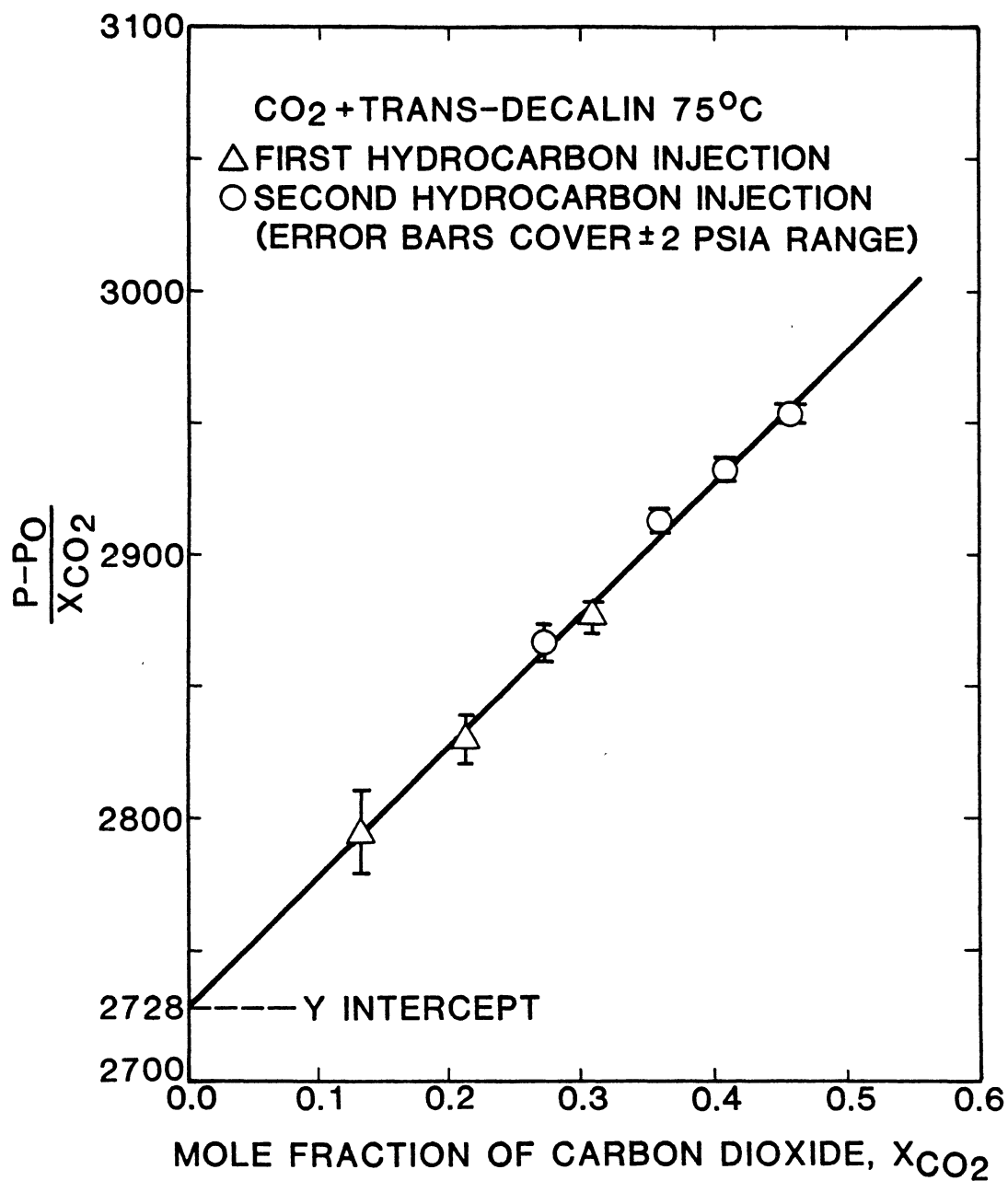


Figure 12. Typical p/x_{CO_2} Versus x_{CO_2} Plot

two separate solvent injections, a check is made on the measurements of the actual amounts of materials injected (both solvent and solute). If an error is made in either injection, the bubble-point pressures will not form a smooth curve when plotted as described above. Another reason the method works so well is that the p/x values cover a range less than p and, in fact, would be constant if Henry's Law was obeyed at all compositions studied.

The above method is a necessary test to be performed on each isotherm. The method, of course, does not guarantee that the data are correct. There is a possibility that the solvent is not properly degassed prior to injection. If this is the case, both solvent injections might match as described above, but the resulting isotherm would still be in error. To check for this occurrence, the solvent should be degassed a second time and then checked using the method as described earlier.

Calibration of Pressure Transducers

The hydrocarbon pressure transducer was calibrated on a regular basis (after each system studied) to assure proper pressure readings during operation. The previously discussed apparatus was designed for easy access to the dead weight gauge, so calibration of the pressure transducers is simple and requires little time. Because the equations used to evaluate the transducer gauge corrections involved numerous repetitive calculations, a computer program was developed (Appendix D) to quickly perform the calculations and determine the transducer corrections. The proper procedure for calibration of the pressure transducers is listed as follows.

1. Using an accurate cathetometer, measure the heights of the transducers (in the injection pump bath), mercury-oil interface, and dead weight gauge reference point. Calculate the head correction from these measured heights to account for the difference in fluid levels between the reference line on the dead weight gauge and the pressure transducers (see Appendix D).

2. Open V10, IV, DW1, DW2, and DW3. Check the mercury level in the Jergusen gauge to make sure it is level with the black reference line marked on the outside cover of the gauge. This black line is the height of the the mercury-oil interface used to calculate the head correction so it is important that the mercury-oil interface is always set at this height. If the mercury level is not even with the black reference mark, open PV1 and adjust the cleaning pump to return the mercury level in the Jergusen gauge to the proper mark. Isolate the cleaning pump by closing PV1 once the mercury-oil interface has been returned to the correct height.

3. Now the dead weight gauge is linked directly to the pressure transducer, and the calibration is begun by placing the appropriate disk weights on the floating piston of the dead weight gauge. The choice of weights depends on the particular pressure range over which the apparatus will be operated. Appendix D shows a useful combination of disk weights and the resulting pressures the various combinations of weights produce. Once the weights have been placed on the gauge, adjust the pump handle on the dead weight gauge so that the reference mark on the floating piston aligns with the reference mark on the piston housing. While keeping the two reference marks aligned, monitor the pressure reading on the pressure transducer readout and record the

pressure when it stabilizes. Change the weight(s), and align the reference marks after each change, then record the corresponding pressure readings.

4. After the desired range of pressures has been covered, return the weights to their respective places in the storage box. Return the floating piston to its original position by reversing the pump of the dead weight gauge until the floating piston rests on the piston housing. Isolate the dead weight gauge from the apparatus by closing valves DW1, DW2, DW3, and IV1. Calculate the transducer gauge corrections using the program mentioned earlier and print out the transducer calibration record. This calibration record is used to correct bubble-point pressures measured with the apparatus. Further information concerning the dead-weight gauge operation and maintenance is found in the manual which accompanies the gauge (24).

*Pressure determination of the gas
and the bubble point
also mention the head requirement of gas in bubble detector
mention oil/meniscus interface*

CHAPTER VI

RESULTS AND DISCUSSION

During the initial stages of this study, primary emphasis was placed on modifying and testing a new phase equilibrium cell. After completing the modifications, the following improvements were observed through operation of the modified cell.

1. Effects of room temperature fluctuations on pressure measurements were eliminated by carefully controlling the temperatures of all critical components.

2. The magnetic stirrer provided much better stirring of the cell contents than the previously used rocking mechanism; in the single-phase region, equilibrium is now attained in 5-10 minutes (where previously it took a minimum of 60 minutes).

3. The pressure transducers (readable to 0.1 psi) provide valuable monitoring of the approach to equilibrium and facilitate detection of leaks in the apparatus.

4. The use of smaller injection pumps (with higher resolution of the injection volumes) permits more precise detection of the bubble-point pressure.

5. Implementation of a valve handle extension for valve OV2 which extends through the cell bath door reduces time required for solvent injection because thermal equilibrium is no longer disturbed by opening the cell bath door to gain access to OV2.

6. By isolating the cell bath contents (solvents that were solids at room temperature) from all lines external to the cell bath, clogging was nearly eliminated. These improvements resulted in an approximate three-fold increase in the rate of data production with equal or higher precision than was previously possible.

To test the modified apparatus and procedures used in this study, several preliminary measurements were made. First, vapor pressures of pure propane and pentane were determined at various temperatures. As shown in Table I, the measured vapor pressures agree well with literature sources, confirming the temperature and pressure measurements of the apparatus. Next, solubility data were measured on the system CO_2 + benzene at 40°C (Table II) because several investigators (1 - 4) had studied this mixture. Comparisons of the various literature values with this work are shown in Figure 13, expressed in terms of the difference between the measured solubility (mole fraction CO_2), $(x_{\text{calc}} - x_{\text{exp}})$, and the prediction of the Soave equation fit to the present data. The data are presented in this form to allow comparison of the various data sets on a much more sensitive scale than is possible using a p vs. x_{CO_2} plot directly. (The deviations shown in Figure 13 would be totally obscured on a p vs. x_{CO_2} plot.) Except for the data of Ohgaki (3) (which appear to be in error), agreement is reasonable among the investigators. These results were taken as confirmation of proper operation of the new apparatus.

After successfully completing measurements of the CO_2 + benzene system, the study was expanded to three other systems (CO_2 + cyclohexane, CO_2 + trans-Decalin, CO_2 + naphthalene). Results of the solubilities measured for these systems are given in Tables III-V. To

TABLE I
PRELIMINARY VAPOR PRESSURE MEASUREMENTS

Temperature (°C)	Experimental Vapor Pressure (psia)		Literature Vapor Pressure* (psia)	
	n-pentane	benzene	n-pentane	benzene
40	17.8	3.9	17.3	3.5
50	24.1	5.4	23.8	5.2

* Literature vapor pressure calculated using Antoine's Equation constants from Reference 25.

TABLE II
SOLUBILITY OF CO₂ IN BENZENE

Mole Fraction CO ₂	Pressure MPa (psia)
-----313.2K (40°C, 104°F)-----	
0.139	1.644 (238.4)
0.181	2.106 (305.5)
0.325	3.544 (514.0)
0.401	4.186 (607.1)
0.500	4.925 (714.3)
0.602	5.572 (808.1)

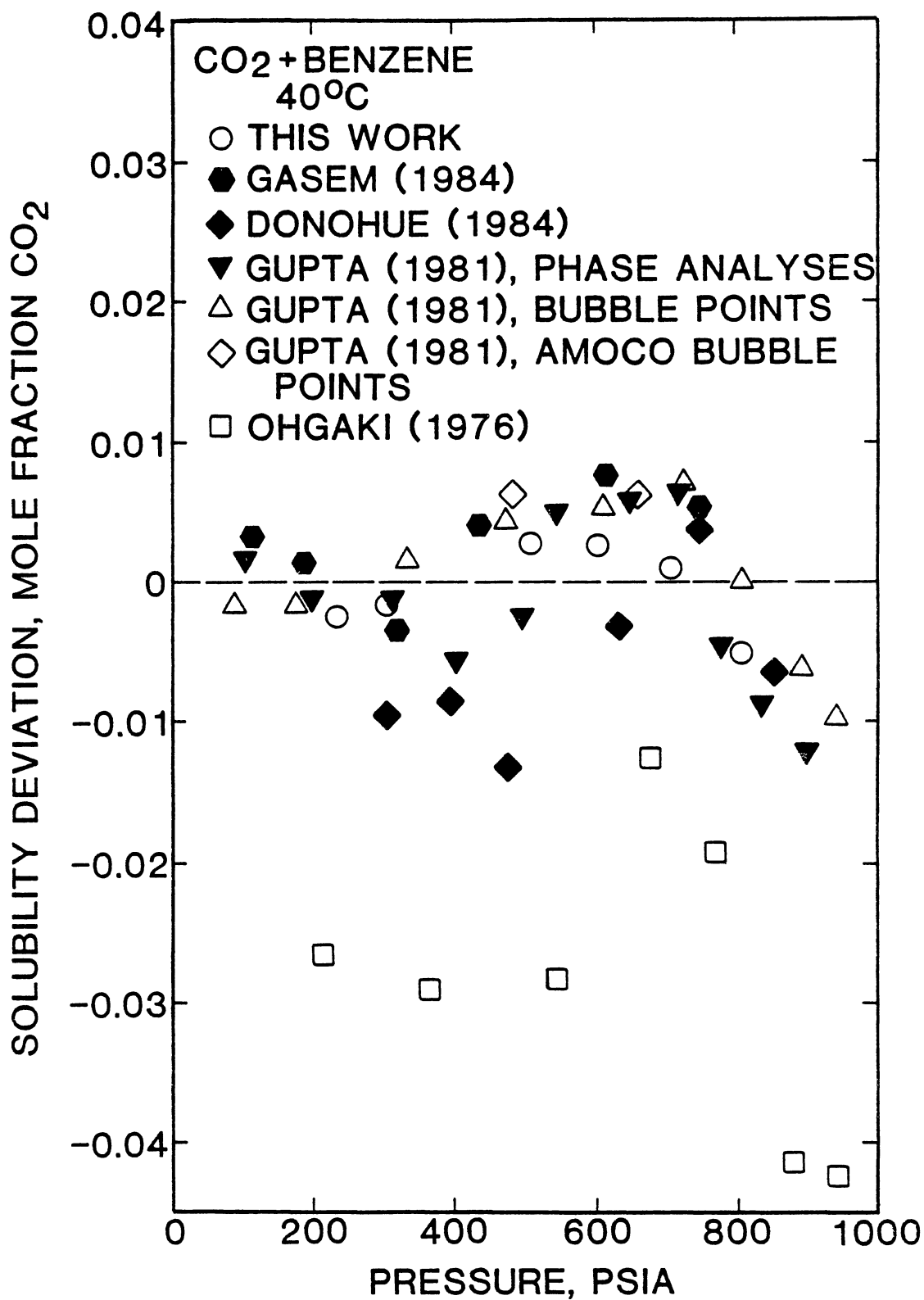


Figure 13. Comparison of Measurements of CO₂ Solubility in Benzene at 40°C

TABLE III
SOLUBILITY OF CO₂ IN TRANS-DECALIN*

Mole Fraction CO ₂	Pressure MPa (psia)	
-----323.2K (50°C, 122°F)-----		
0.093	1.576	(228.6)
0.170	2.899	(420.5)
0.243	4.137	(600.0)
0.300	5.103	(740.1)
0.351	5.928	(859.8)
0.399	6.729	(976.0)
-----348.2K (75°C, 167°F)-----		
0.133	2.553	(370.3)
0.139	2.688	(389.8)
0.214	4.172	(605.1)
0.224	4.337	(629.0)
0.273	5.388	(781.5)
0.310	6.138	(890.2)
0.325	6.453	(935.9)
0.360	7.223	(1047.6)
0.408	8.240	(1195.1)
0.456	9.295	(1348.1)
-----373.2K (100°C, 212°F)-----		
0.098	2.184	(316.7)
0.161	3.645	(528.7)
0.193	4.376	(634.7)
0.254	5.932	(860.4)
0.322	7.641	(1108.3)
0.360	8.632	(1252.0)
0.422	10.297	(1493.4)

TABLE III (Continued)

Mole Fraction CO ₂	Pressure	
	MPa	(psia)
-----423.2K (150°C, 302°F)-----		
0.052	1.469	(213.0)
0.103	2.962	(429.6)
0.144	4.172	(605.1)
0.199	5.861	(850.0)
0.250	7.475	(1084.1)
0.295	8.963	(1300.0)
0.345	10.657	(1545.7)

* For the 323.2K isotherm, the solvent is a mixture of cis- and trans-Decalin.

TABLE IV
SOLUBILITY OF CO₂ IN CYCLOHEXANE

Mole Fraction CO ₂	Pressure	
	MPa	(psia)
-----348.2K (75°C, 167°F)-----		
0.103	1.979	(287.0)
0.173	3.283	(476.2)
0.302	5.407	(784.2)
0.399	6.782	(983.7)
0.505	8.150	(1182.0)
0.577	9.000	(1305.4)
-----373.2K (100°C, 212°F)-----		
0.126	2.841	(412.1)
0.183	3.994	(579.3)
0.210	4.558	(661.1)
0.308	6.465	(937.7)
0.350	7.244	(1050.6)
0.403	8.209	(1190.6)
0.507	9.995	(1449.6)

TABLE IV (Continued)

Mole Fraction CO ₂	Pressure	
	MPa	(psia)
-----423.2K (150°C, 302°F)-----		
0.112	3.403	(493.5)
0.160	4.616	(669.5)
0.200	5.610	(813.6)
0.257	7.015	(1017.4)
0.300	8.079	(1171.7)
0.350	9.249	(1341.4)
0.401	10.428	(1512.4)

TABLE V
SOLUBILITY OF CO₂ IN NAPHTHALENE

Mole Fraction CO ₂	MPa	Pressure (psia)
-----373.2K (100°C, 212°F)-----		
0.047	1.385	(200.9)
0.107	3.196	(463.5)
0.133	3.978	(577.0)
0.162	4.852	(703.7)
0.202	6.091	(883.4)
0.248	7.586	(1100.2)
0.336	10.451	(1515.8)
-----433.2K (150°C, 302°F)-----		
0.051	1.925	(279.2)
0.107	4.129	(598.9)
0.110	4.229	(613.4)
0.151	5.873	(851.8)
0.201	7.879	(1142.8)
0.224	8.845	(1282.9)
0.252	9.965	(1445.2)

give a general indication of the effect of temperature on the measured solubilities, Figure 14 shows a typical p vs x_{CO_2} plot for the CO_2 + cyclohexane system at 75, 100, and 150°C.

As a supplement to the data, of the present work, the densities used in this study and the corresponding moles of solvent and solute injected measurements are shown in Table VI. This information may be used to adjust the solubilities reported in Table III-V if more accurate data for pure component properties become available (relative to those given in Table VI). Use of Table VI to recalculate solubilities is explained in Appendix E.

Figure 15 shows a comparison of the solubilities at 75°C of CO_2 in the aromatic solvent benzene (interpolated from the data of Gupta, et al. (2)) with the solubilities of CO_2 in the naphthenic solvent cyclohexane (this work) and the n-paraffin solvent n-hexane (interpolated from the data of Li, et al., (27)). As indicated in Figure 15, the solubilities of CO_2 in the aromatic solvent are slightly higher (approximately 4%) than those in the naphthenic solvent. These results are in agreement with Mundis (11) and Battino (7), who found that CO_2 is more soluble in aromatic solvents than in naphthenic solvents having the same number of carbon atoms. In contrast to results for CO_2 solubilities in these six-carbon solvents, Figure 16 reveals that an increase in solvent carbon number reverses the effect of molecular structure on the CO_2 solubility. Here the solubility of CO_2 in the aromatic solvent (naphthalene) is as much as 21% lower than in the naphthenic solvent (trans-Decalin). Further inspection of Figure 16 shows that the solubility of CO_2 in the n-paraffin solvent n-decane (Reamer and Sage (28)) are much higher than those of CO_2 in either the

TABLE VI
DENSITIES AND VOLUMES USED TO CALCULATE
SOLUBILITIES FOR THIS STUDY

Solvent Density (g/cc)	Gram Moles of Solvent Injected	Injection Pressure for CO ₂ at 50°C (psia)	Calculated CO ₂ density (g/cc)	Total Gram Moles of Solute Injected	Solvent Injection	
-----Benzene 40°C-----						
0.8577	0.07466	589.3	0.082895	0.01204	1	
		589.3		0.03599	1	
		595.6		0.05003	1	
	0.04546	576.7	0.083898	0.01005	2	
		0.07749	748.2	0.080776	0.07744	3
			748.2	0.109127	0.11736	3
-----Cis/Trans-Decalin 50°C-----						
0.8450	0.045382	588.9	0.080332	0.00929	1	
		588.9		0.01947	1	
		588.9		0.03008	1	
	0.051342	588.9	0.00524	2		
		588.9	0.01644	2		
		588.9	0.02771	2		
-----Trans-Decalin 75°C-----						
0.8240	0.04065	780.8	0.115910	0.00621	1	
		780.8		0.01106	1	
		780.8		0.01822	1	
	0.05047	770.1	0.113716	0.01891	2	
		770.1	0.02835	2		
		770.1	0.03471	2		
770.1	0.04238	2				
-----Trans-Decalin 100°C-----						
0.8124	0.03956	770.0	0.113716	0.00947	1	
		770.0		0.01877	1	
		770.0		0.02222	1	
		770.0		0.02885	1	
	0.04180	788.7	0.117577	0.00454	2	
		788.7	0.00801	2		
788.7	0.01426	2				

TABLE VI (Continued)

Solvent Density (g/cc)	Gram Moles of Solvent Injected	Injection Pressure for CO ₂ at 50°C (psia)	Calculated CO ₂ density (g/cc)	Total Gram Moles of Solute Injected	Solvent Injection
-----Trans-Decalin 150°C-----					
0.7865	0.04061	752.7	0.109783	0.01034	1
		752.7		0.01736	1
		752.7		0.02186	1
	0.04583	783.7	0.116458	0.00249	2
		783.7		0.00525	2
		783.7		0.00786	2
		783.7		0.01525	2
-----Cyclohexane 75°C-----					
0.71930	0.05409	592.4	0.080932	0.01128	1
		592.4		0.02336	1
		592.4		0.03594	1
	0.05799	593.8	0.081107	0.00663	2
		824.7		0.124923	2
		1145.4		0.213318	2
		1145.4		0.07914	2
-----Cyclohexane 100°C-----					
0.69555	0.05429	825.3	0.125108	0.00780	1
		825.3		0.01444	1
		825.3		0.02411	1
	0.05220	806.1	0.120976	0.01170	2
		806.1		0.02812	2
		806.1		0.03523	2
		806.1		0.05364	2
-----Cyclohexane 150°C-----					
0.64740	0.05006	768.5	0.113297	0.00629	1
		768.5		0.01248	1
		768.5		0.01727	1
	0.05265	773.1	0.114225	0.00999	2
		773.1		0.02253	2
		773.1		0.02829	2
		773.1		0.03518	2

TABLE VI (Continued)

Solvent Density (g/cc)	Gram Moles of Solvent Injected	Injection Pressure for CO ₂ at 50°C (psia)	Calculated CO ₂ density (g/cc)	Total Gram Moles of Solute Injected	Solvent Injection
-----Naphthalene 100°C-----					
0.9628	0.05063	693.4	0.098934	0.00778	1
		693.4		0.01667	1
		693.4		0.02567	1
	0.054863	756.9	0.111168	0.00270	2
		756.9		0.00659	2
		756.9		0.01065	2
		756.9		0.01387	2
-----Naphthalene 150°C-----					
0.9219	0.054301	670.9	0.094788	0.00293	1
		670.9		0.00668	1
		670.9		0.01363	1
	0.04112	742.3	0.108282	0.00492	2
		742.3		0.00731	2
		742.3		0.01188	2
		742.3		0.01380	2

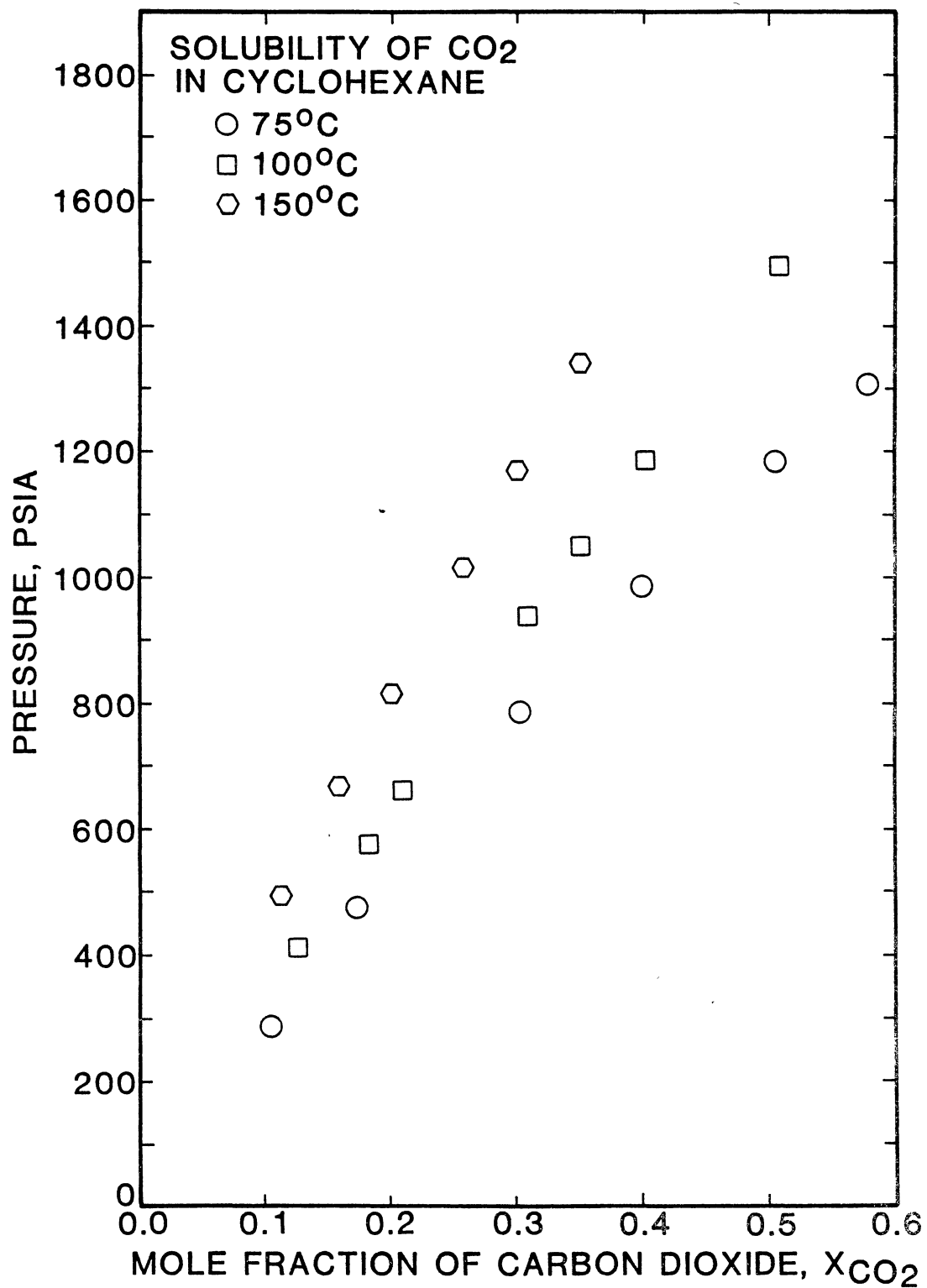


Figure 14. The Effect of Temperature on CO₂ Solubility in Cyclohexane

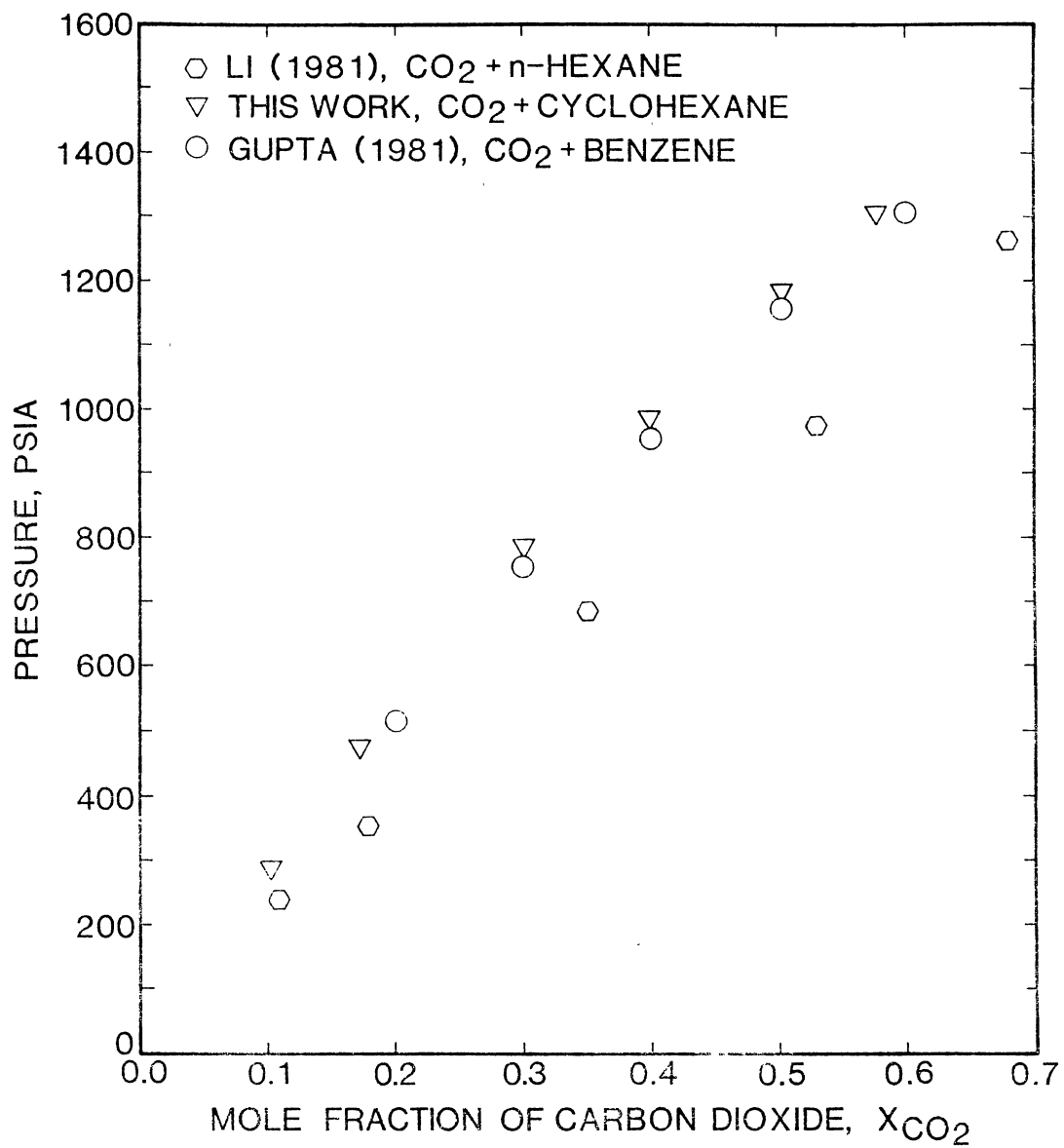


Figure 15. The Effect of Molecular Structure on CO₂ Solubility in Six-Carbon Solvents

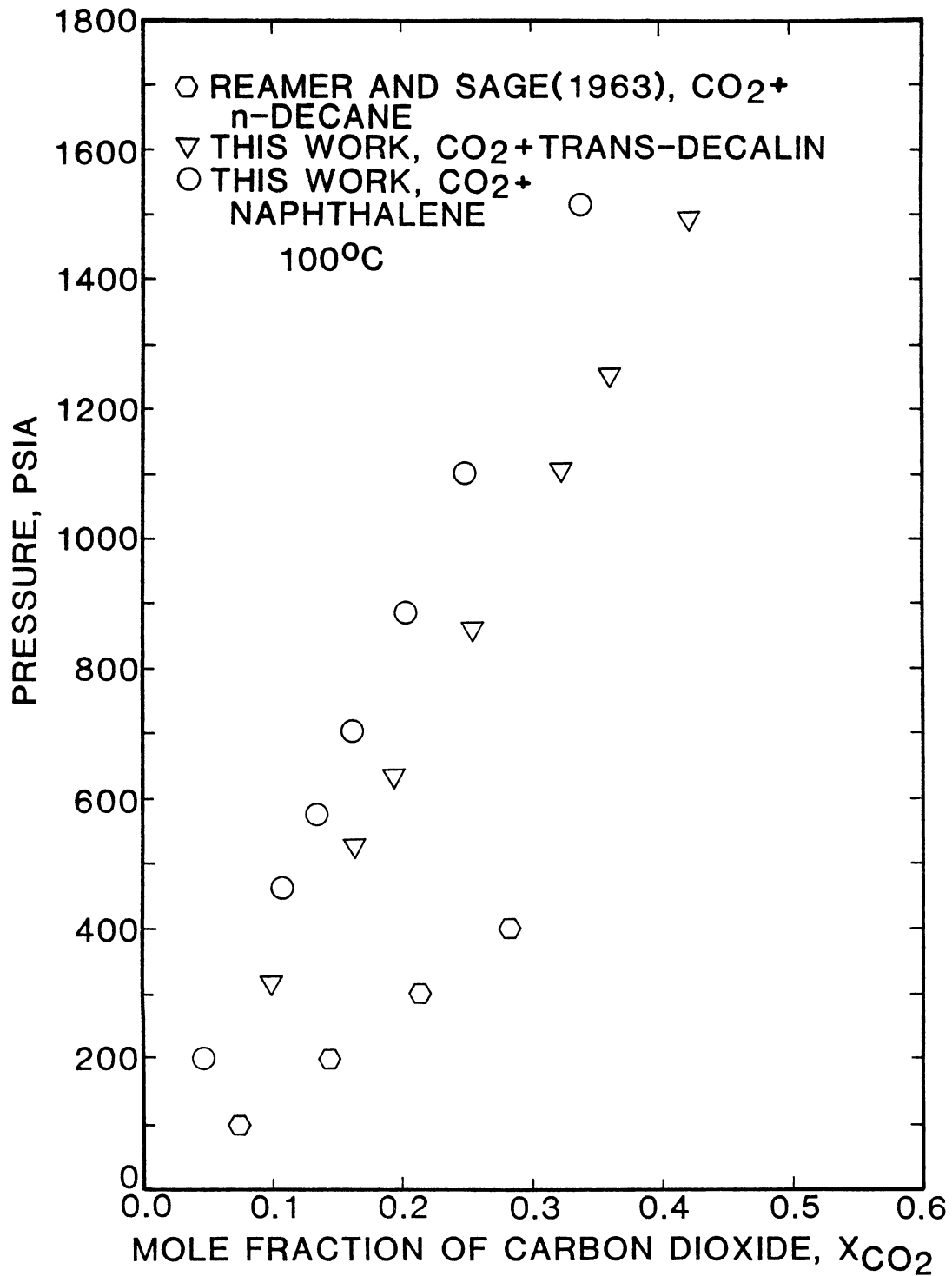


Figure 16. The Effect of Molecular Structure on CO₂ Solubility in Ten-Carbon Solvents

aromatic or naphthenic solvents.

In a manner similar to Figure 13 for CO₂ + benzene, Figure 17 shows results for CO₂ + trans-Decalin and CO₂ + cyclohexane. The deviations are based on fit of the Soave equation to the individual isotherms, and the Soave parameters (k_{ij} , l_{ij}) are given in Table VII. With the exception of the 75°C cyclohexane isotherm, these figures show that the scatter in the experimental results appears to be near the expected experimental uncertainty of 0.0004 in CO₂ mole fraction.

Figure 18 presents a comparison of the results of Tiffin, et al. (9) with the present work for CO₂ + trans-Decalin at 75°C. Significant deviations are evident between the two data sets. In fact, because the deviations were so significant, a third run was made from scratch after the solvent had been degassed extensively for the second time to assure that the data on this system was measured correctly. These additional measurements substantiate the present work as shown in Figure 18. Better agreement is shown between the data of Tiffin, et al. at 50°C and present measurements in mixed cis/trans-Decalin (the solvent used was an equimolar mixture of cis-Decalin and trans-Decalin) at the same temperature (Figure 19), however slight deviations are still evident and cannot be explained at the present time.

Figure 20 shows the deviations of the CO₂ + naphthalene system based on the fit of the Soave equation of state to the individual isotherms. Each hydrocarbon injection is shown individually to demonstrate the repeatability of solubility measurements taken from separate solvent injections. Although no literature data are available for comparison, Table VII shows that interaction parameters regressed

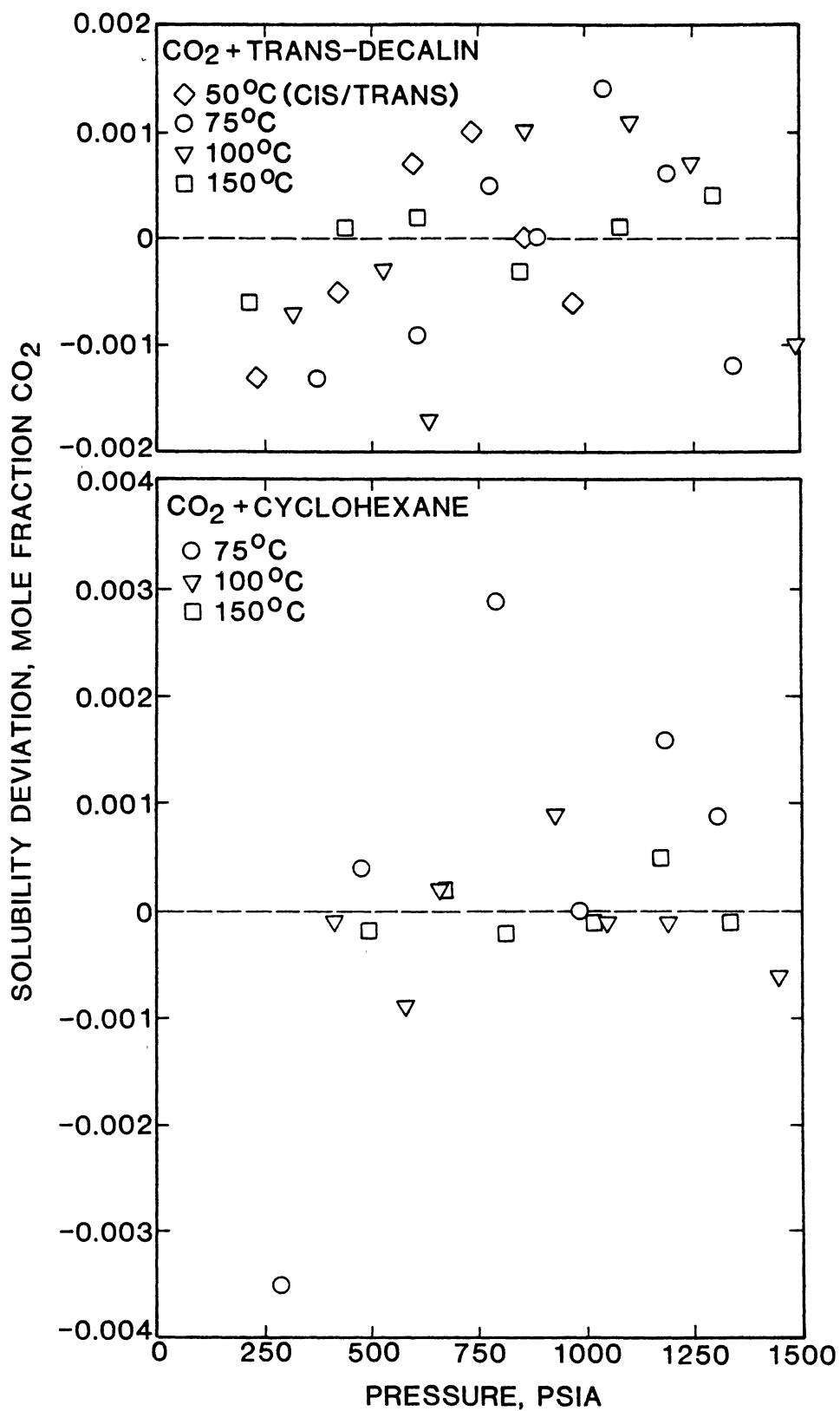


Figure 17. Soave Equation Representations of CO₂ Solubilities in trans-Decalin and Cyclohexane

TABLE VII
 SOAVE AND PENG-ROBINSON EQUATION OF STATE
 REPRESENTATIONS OF CO₂ SOLUBILITY DATA

Temperature K(°F)	Soave Parameters (P-R Parameters)		Error in CO ₂ * Mole Fraction	
	k ₁₂	l ₁₂	RMS	Max.
-----CO ₂ + Benzene-----				
313.2 (104)	0.068	0.035	0.003	0.005
	(0.066)	(0.037)		
	0.090	--	0.018	0.031
	(0.089)	--		
-----CO ₂ + Trans-Decalin-----				
323.2 (122)*	0.145	0.030	0.001	0.001
	0.181	--	0.011	0.015
348.2 (167)	0.137	0.025	0.001	0.001
	(0.125)	(0.027)		
	0.167	--	0.009	0.012
	(0.153)			
373.2 (212)	0.143	0.022	0.001	0.002
	(0.129)	(0.023)		
	0.168	--	0.006	0.008
	(0.155)			
423.2 (302)	0.156	0.020	< 0.001	0.001
	(0.140)	(0.019)		
	0.183	--	0.003	0.004
	(0.165)			
348.2, 373.2 and 423.2	0.136	0.029	0.004	0.010
	(0.126)	(0.027)		
	0.168	--	0.009	0.020
	(0.156)			

TABLE VII (Continued)

Temperature K(°F)	Soave Parameters (P-R Parameters)		Error in CO ₂ ** Mole Fraction	
	k ₁₂	l ₁₂	RMS	Max.
-----CO ₂ + Cyclohexane-----				
348.2 (167.0)	0.108	0.051	0.002	0.004
	(0.099)	(0.053)		
	0.136	--	0.020	0.027
	(0.128)			
373.2 (212.0)	0.113	0.042	0.001	0.001
	(0.102)	(0.043)		
	0.141	--	0.011	0.019
	(0.131)			
423.2 (302.0)	0.125	0.034	< 0.001	0.001
	(0.111)	(0.033)		
	0.151	--	0.005	0.007
	(0.136)			
348.2, 373.2 and 423.2	0.112	0.046	0.003	0.007
	(0.102)	(0.044)		
	0.141	--	0.014	0.038
	(0.131)			
-----CO ₂ + Naphthalene-----				
373.2 (212)	0.079	0.027	0.001	0.001
	(0.075)	(0.030)		
	0.118	--	0.007	0.009
	(0.116)	--		
423.2 (302)	0.068	0.031	< 0.001	< 0.001
	(0.064)	(0.032)		
	0.119	--	0.004	0.005
	(0.115)	--		
373.2 and 423.2	0.082	0.024	0.002	0.004
	(0.079)	(0.025)		
	0.119	--		
	(0.116)	--		

* The RMS and maximum errors in CO₂ mole fraction are essentially the same for both the Soave and Peng-Robinson equations of state.

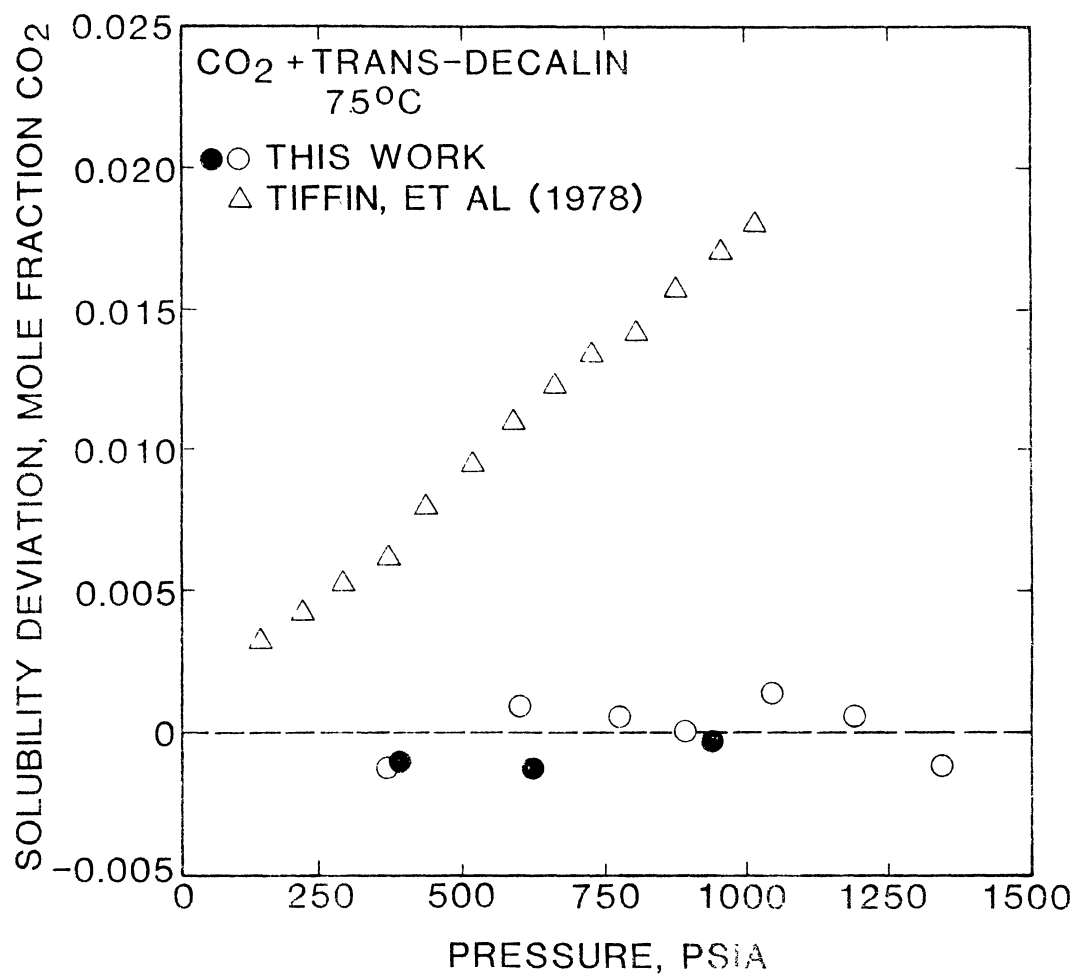


Figure 18. Comparison of Data for CO₂ Solubility in trans-Decalin at 75°C

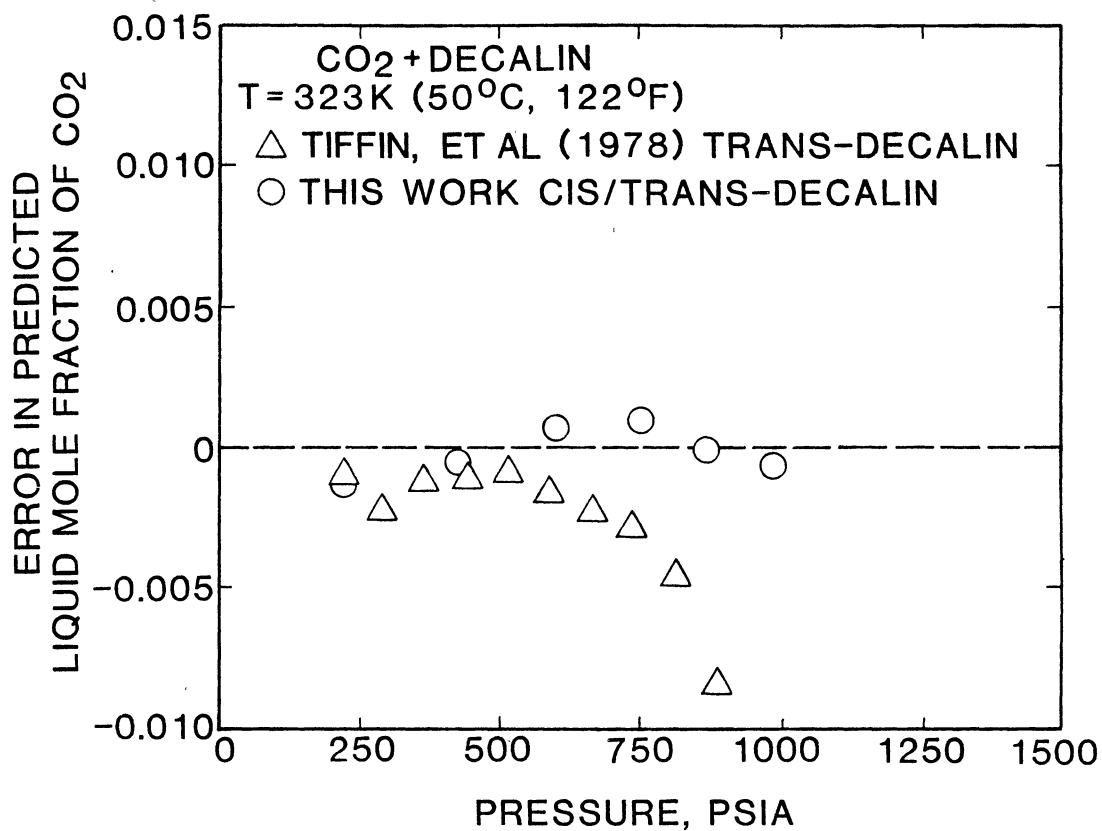


Figure 19. Comparison of Data for CO₂ Solubility in Decalin at 50°C

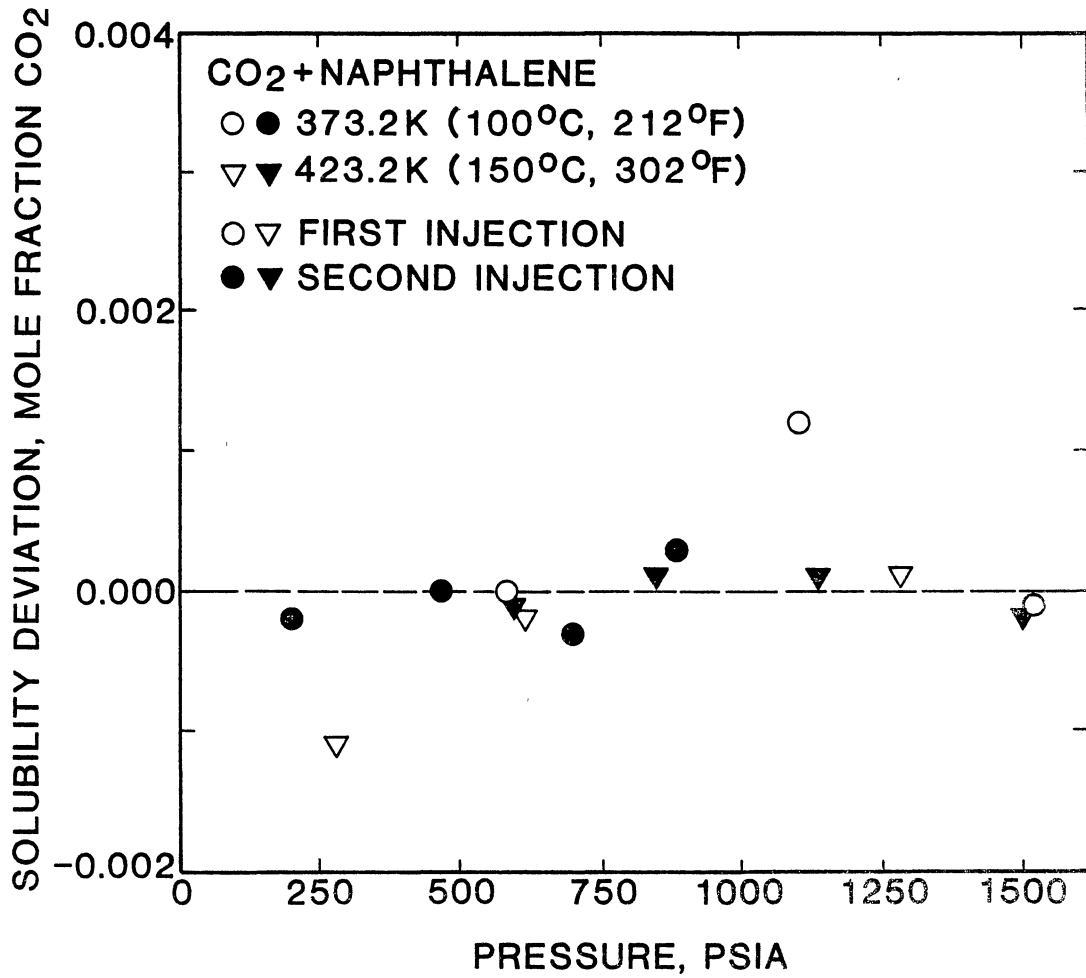


Figure 20. Soave Equation Representation of CO₂ Solubility in Naphthalene

from the CO₂ + naphthalene solubility measurements follow the same trend of aromatic solvent behavior demonstrated by comparison of the benzene and cyclohexane systems (i.e., k_{ij} for aromatic solvents is lower than k_{ij} for naphthenic solvents of the same carbon number).

The values in Table VII also confirm the suggestion of Turek (14) that two interaction parameters are required for CO₂ systems. Use of a single interaction parameter (k_{ij}) results in a significant increase in errors in predicted solubilities. Further review of the k_{ij} and l_{ij} parameters in Table VII reveals a definite temperature dependence for both parameters; however, treating the parameters as temperature independent still gives reasonably acceptable results (RMS error in CO₂ mole fraction increases to 0.011). These findings are in agreement with Lin, who suggests there is no need to treat k_{ij} as temperature dependent, although he does state that the best results are achieved by using optimum values of k_{ij} obtained by fit to each individual isotherm (13).

Figure 21 shows values of k_{ij} and l_{ij} respectively as a function of temperature for the CO₂ + trans-Decalin system. Both k_{ij} and l_{ij} for this work are in reasonable agreement with the values regressed from the data of Tiffin, et al. (An arbitrary error bar of ± 0.005 was attached to each interaction parameter). The figures again establish that both k_{ij} and l_{ij} are temperature dependent.

Figures 22 and 23 compare values of k_{ij} and l_{ij} , respectively, as functions of temperature for the CO₂ + cyclohexane system. A comparison of k_{ij} and l_{ij} was used to compare data because the temperature ranges used in the literature data do not correspond to the ranges used in this

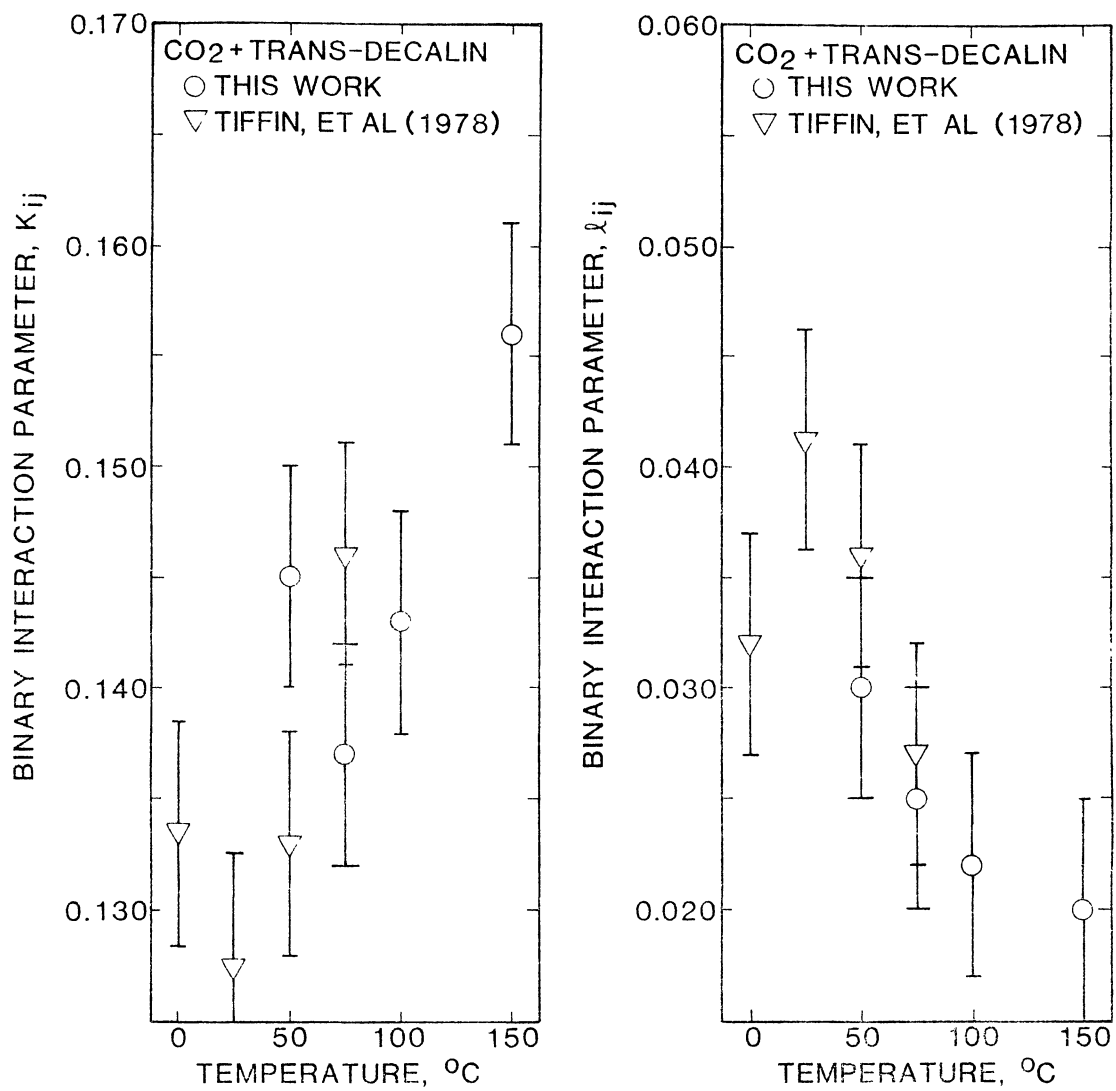


Figure 21. Effect of Temperature on Interaction Parameters for CO_2 + trans-Decalin

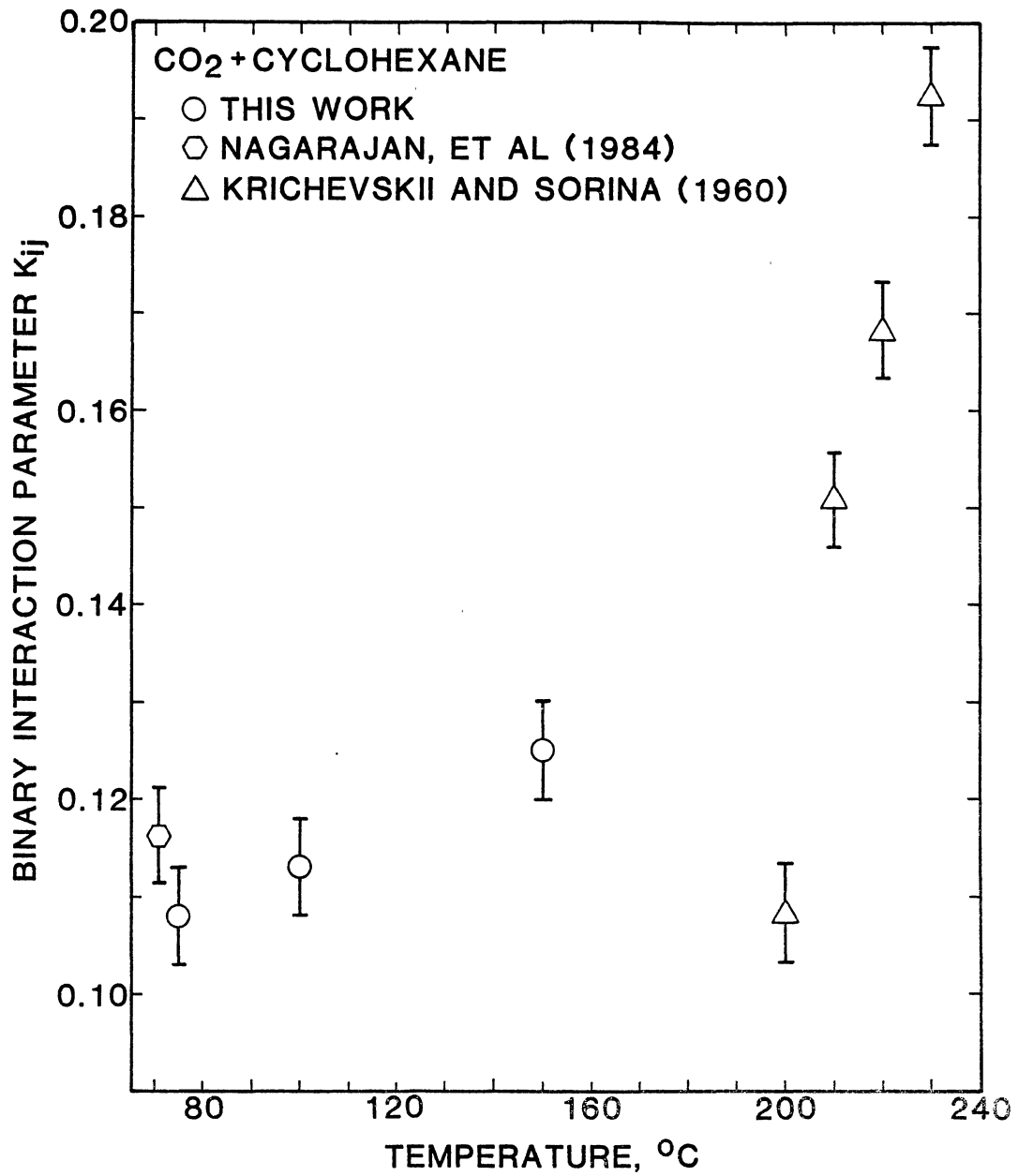


Figure 22. Effect of Temperature on k_{ij} for CO₂ + Cyclohexane

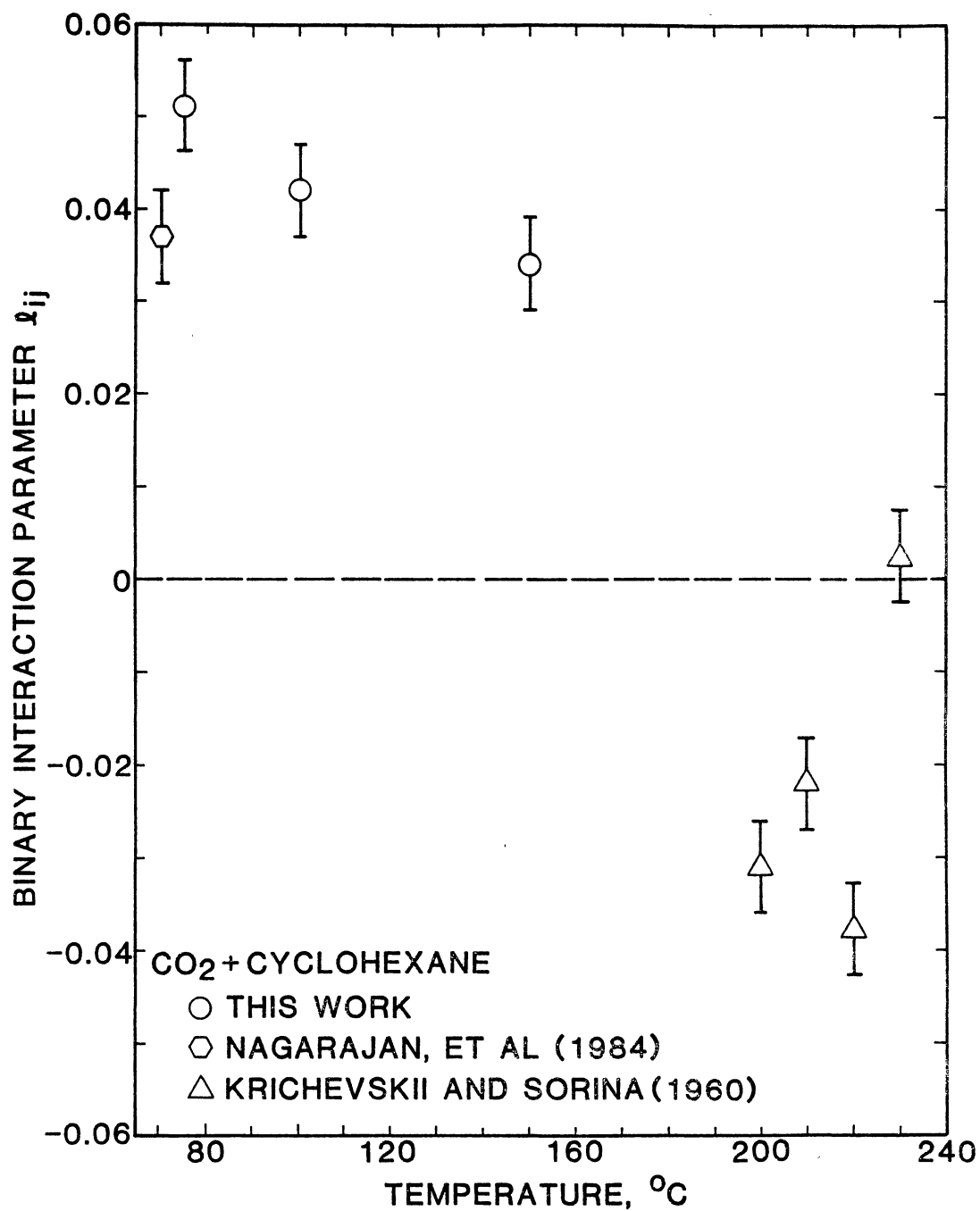


Figure 23. Effect of Temperature on l_{ij} for CO₂ + Cyclohexane

work. The data in Figure 22 show the k_{ij} values regressed from the data of both Nagarajan (8) and Krichevskii and Sorina (5) to be in reasonable agreement with values calculated from this work; however, the data of Krichevskii and Sorina show considerable scatter in Figure 23 which raises some doubt as to their precision.

Although the interests of this work are primarily in high pressure solubilities, an attempt was made to predict some low pressure (atmospheric) solubilities from the acquired data, so a comparison could be made with low pressure solubilities published by Dymond (6) and by Wilhelm and Battino (7). By extrapolating the p/x vs x plots for each isotherm of the CO_2 + cyclohexane system (as demonstrated in Figure 12 for the CO_2 + trans-Decalin system) back to zero mole fraction of carbon dioxide (i.e., taking the "y-intercept" of each plot), low pressure solubilities were determined for comparison with the literature values. Predicted low pressure solubilities from this work are shown in Figure 24 as a function of the inverse of the absolute temperature. These solubilities seem to follow the same trend as the literature data, which suggests that the predicted values are acceptable and, thus, provides further evidence that the acquired data are a good representation of the CO_2 + cyclohexane system.

Of final interest is a comparison of the results calculated using the Peng-Robinson and Soave equations of state. Results in Table VII confirm the abilities of both the Soave and Peng-Robinson equations of state to represent the data to essentially their experimental accuracies when two binary interaction parameters are used per isotherm. (Errors in the calculated solubilities approach the expected experimental error level of approximately 0.001 mole fraction when both parameters are used

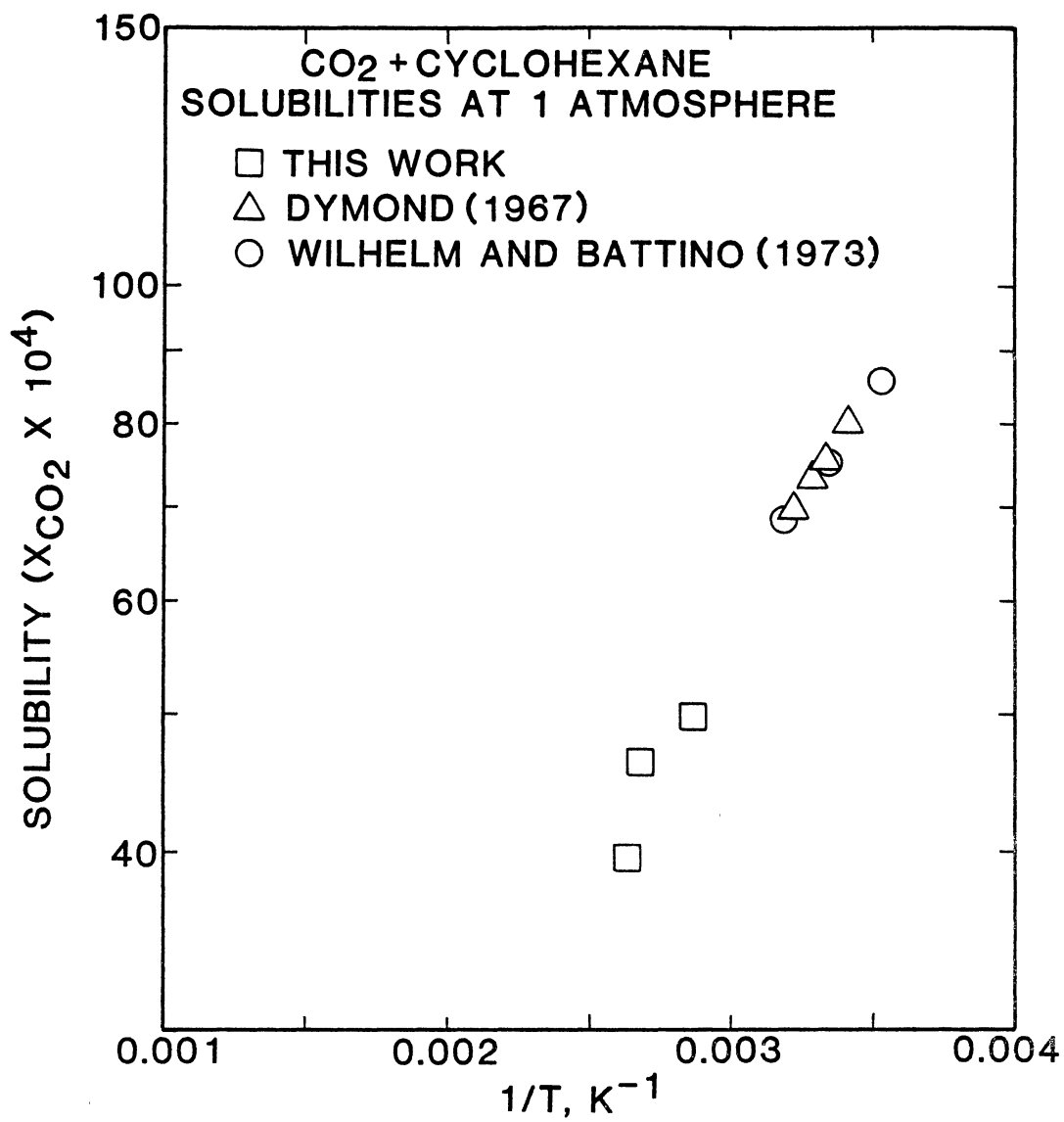


Figure 24. Comparison of Solubility Data at one Atmosphere for CO₂ + Cyclohexane

for each isotherm.) As indicated in Table VII, there is virtually no difference in the error in CO₂ mole fraction calculated from the two equations; thus, errors are shown only for the Soave equation. As no general correlation was evident for either k_{ij} or l_{ij} as a function of temperature, no attempt was made to correlate them as such; however, both l_{ij} and k_{ij} show the same temperature dependent trends for each equation of state. There is a systematic variation between the k_{ij} values regressed from the Soave equation and those regressed from the Peng-Robinson equation (l_{ij} is essentially the same for both cases). For the two naphthenic systems (CO₂ + trans-Decalin, CO₂ + cyclohexane), k_{ij} from the Soave equation is consistently approximately 0.011 larger than k_{ij} from the Peng-Robinson equation; while for the two aromatic systems (CO₂ + benzene, CO₂ + naphthalene), k_{ij} from the Soave equation is consistently approximately 0.003 larger than k_{ij} from the Peng-Robinson equation.

Problems Encountered During Operation of Apparatus

Although extensive planning was used to properly design the new apparatus, some operational problems began to surface after long-term use of the equipment. These problems and suggestions for improving them are discussed in the following section.

The most time consuming problem was caused by a poor choice of materials. Bearings which were used to support the magnetic drive wheel inside the cell bath would seize at temperatures above 100°C and deform the track around the drive wheel. After extensive use, the drive wheel became deformed to such an extent that it had to be replaced, slowing experimentation considerably. This problem should be fixed easily by

using bearings with a higher temperature rating or a drive wheel with a protected track.

Another problem encountered during operation of the modified apparatus was caused by faulty design. Although the apparatus was specially designed to handle solvents which were solid at room temperature, plugs still formed in lines extending from the cell bath which were exposed to room temperature. The plugs were eventually removed by applying direct heat with a heat gun; however, several minutes were required to do so. The solution to this problem is to reroute all lines external to the cell bath which contain solvents that are solids at room temperature in such a manner that a minimum of tubing surface area is exposed to room temperature.

A second design problem was found in the cell cleaning system. Because of the restricted flow area of 1/16" tubing used in the cleaning system, cleaning fluid could not flow readily from the cleaning fluid reservoir to the cleaning fluid storage cylinder (at times requiring 20 minutes for 70 cc to flow from the reservoir to the cylinder). Since the cleaning system was used two to three times daily, experimentation was slowed by over an hour due to the restricted flow of the cleaning fluid. By replacing the 1/16" tubing with 1/8" tubing, flow area could be increased and the cleaning fluid could travel faster through the cleaning system.

CHAPTER VII

CONCLUSIONS AND RECOMMENDATIONS

Conclusions

1. Data have been obtained which display quantitatively the relative effects of naphthenic and aromatic solvents on the high pressure solubilities of CO₂.
2. These data are represented adequately by both the Soave and Peng-Robinson equations of state using two binary interaction parameters, k_{ij} and l_{ij} , for each binary system; average errors in the predicted solubility of CO₂ are on the order of 0.001 at CO₂ mole fractions up to 0.600.
3. Both k_{ij} and l_{ij} show dependence on temperature; however, before a proper correlation can be developed, more data at different temperatures must be produced.
4. Using a single set of parameters to represent each CO₂ + hydrocarbon system over a temperature range of 50 to 150°C permits predictions with reasonable accuracy in predicted CO₂ solubility; the maximum increase in error was from 0.001 RMS error to 0.004 RMS error.
5. The information presented herein can be used to predict phase behavior of multicomponent fluids containing naphthenic and aromatic solvents.
6. The modified solubility apparatus worked well. Not only was data acquisition increased to three times the original rate, but

accuracies in measurement of the CO₂ solubility and bubble-point pressure were increased to ± 0.001 and ± 1.4 psia respectively.

7. Maintenance of the apparatus became more efficient and safety was improved as less time was spent handling hazardous materials.

Recommendations

1. Further studies should be done on naphthenic and aromatic solvents with higher carbon number (i.e. phenanthrene, pyrene, tetralin, etc.) as well as on mixed solvents containing both sufficient naphthenic and aromatic components. Such studies will provide data so that a systematic comparison can be made between aromatic and naphthenic solvent behavior for the heavier constituents of coal fluids. Study of mixed solvents will give greater knowledge of actual hydrocarbon + hydrocarbon interaction which may occur in coal fluids.

2. Because of solvents solidifying in lines outside of the cell bath, all such lines should be rerouted to achieve a minimum of exposed line surface area.

3. Bearings which operate freely at temperatures above 150°C should be used to replace present bearings which tend to seize at temperatures higher than 100°C. Also, a harder material should be used to manufacture the drive wheel which supports the rotating magnets.

4. All 1/16" lines used in the cleaning system should be replaced by 1/8" lines to increase flow rate of mercury through the cleaning system.

REFERENCES

1. Donohue, Marc D., Personal Communication, Johns Hopkins University, Baltimore, Maryland, July 10, 1984.
2. Gupta, M. K., Y.-H. Li, B. J. Hulsey, and R. L. Robinson, Jr., J. Chem. Eng. Data, 27 (1982) 55-57.
3. Ohgaki, K., and T. Katayama, J. Chem. Eng. Data, 21 (1976) 53-55.
4. Gasem, K. A., Ph.D. Dissertation, Oklahoma State University, Stillwater, Oklahoma (in preparation), 1985.
5. Krichevskii, I. R., and G. A. Sorina, Russian J. Phys. Chem., 34 (1960) 679-681.
6. Dymond, J. H., J. Phys. Chem., 71 (1967) 1829-1931.
7. Wilhelm, Emmerich, and Rubin Battino, J. Chem. Eng. Data, 5 (1973) 117-120.
8. Nagarajan, N., Y.-K. Chen, and Robert L. Robinson, Jr. Interfacial Tensions in Carbon Dioxide - Hydrocarbon Systems: Development of Experimental Facilities and Acquisition of Experimental Data. Experimental Data for CO₂ + Benzene. Progress Report to Amoco Production Co., Stillwater, Oklahoma, 1984.
9. Tiffin, D. L., A. DeVera, K. D. Luks, and J. P. Kohn, J. Chem. Eng. Data, 23 (1978) 45-47.
10. Graboski, Michael S., and Thomas E. Daubert, Ind. Eng. Chem. Process Des. Dev., 17 (1978) 448-454.
11. Mundis, C. J., L. Yarborough, and R. L. Robinson, Jr., Ind. Eng. Chem., Process Des. Dev., 16 (1977) 254-259.
12. Huron, Marie-Jose, Gery-Noel Dufarm, and Jean Vidal, Fluid Phase Equilibria, 1 (1977/1978) 247-265.
13. Lin, Ho-Mu, Fluid Phase Equilibria, 16 (1984) 151-169.
14. Turek, E. A., R. S. Metcalfe, L. Yarborough, and R. L. Robinson, Jr., Society of Petroleum Engineers Journal, (1984) 308-324.

15. Yarborough, L., "Application of a Generalized Equation of State to Petroleum Reservoir Fluids" in Equations of State in Engineering, Advances in Chemistry Series, 182, K. C. Chao and R. L. Robinson, Jr., editors, American Chemical Society, Washington, D.C. (1979).
16. Robinson, R. L., Jr., "Review of Phase Equilibrium Thermodynamics", Class Notes, CHENG 5743, Oklahoma State University, Spring, 1984.
17. Modell, M., and R. C. Reid, "Thermodynamics and Its Applications", Prentice Hall, Inc., Englewood Cliffs, N.J., 1974, p. 201.
18. Soave, G., Chem. Eng. Sci., 27 (1972) 1197-1203.
19. Peng, D. Y., and D. B. Robinson, Ind. Eng. Chem., Process Des. Dev., 15 (1976) 59-64.
20. Malanowski, S., Fluid Phase Equilibria, 9 (1982) 311-317.
21. Eubank, P. T., K. R. Hall, and J. C. Holste, "A Review of Experimental Techniques for Vapor-Liquid Equilibria", in 2nd Int. Conf. on Phase Equilibria and Fluid Properties in Chemical Industry. H. Knapp and S. I. Sandler (Editors), DECHEMA, Frankfurt, Part II, 675-687 (1980).
22. Sage, B. H., J. G. Schaffsma, and W. N. Lacey, Ind. Eng. Chem., 26 (1934) 1218-1224.
23. Angus, S., B. Armstrong, and K. M. de Rueck. International Thermodynamic Tables of the Fluid State - 3. Carbon Dioxide, Pergamon Press, Oxford, 1973.
24. Miks, C. E., "Test Report, Ruska Dead Weight Gauge" (Cat. No. 2400.1, Serial No. 10381) Ruska Instrument Co., Houston, Texas, 1963.
25. "Lange's Handbook of Chemistry", 12th ed., John A. Dean, editor, McGraw-Hill Book Co., New York, 1979.
26. Barrick, M. W., M.S. Thesis, Oklahoma State University, Stillwater, Oklahoma (in preparation), 1985.
27. Li, Y.-H., K. H. Dillard, and R. L. Robinson, Jr., J. Chem. Eng. Data, 26 (1981) 53-55.
28. Reamer, H. H., and B. H. Sage, J. Chem. Eng. Data, 8 (1963) 508-513.

APPENDIXES

APPENDIX A

ERROR PROPAGATION IN CO₂ MOLE FRACTION

The mole fraction of component 1, x_1 , in a binary mixture is expressed as:

$$x_1 = \frac{n_1}{n_1 + n_2} \quad (A)$$

The total moles injected for component 1, n_1 , is defined as

$$n_1 = \sum_i \rho_{i1} V_{i1} \quad (B)$$

where

ρ_{i1} = density of component 1 at the temperature and pressure of injection "i"

V_{i1} = volume of component 1 injected during injection "i" as measured from the gas injection pump.

The total moles of component 2 injected is similarly defined as

$$n_2 = \rho_2 V_2 \quad (C)$$

where

ρ_2 = density of component 2 at the temperature and pressure at which component 2 is injected

V_2 = volume of component 2 injected as measured from the hydrocarbon injection pump.

Assuming all of the component 1 injections are made at the same temperature and pressure, substitution of Equations (B) and (C) into Equation (A) yields

$$x_1 = \frac{\rho_1 \sum V_{i1}}{\rho_1 \sum V_{i1} + \rho_2 V_2} \quad (D)$$

The uncertainty in the mole fraction of component 1, σ_{ρ_1} , can be defined as

$$\begin{aligned} \sigma_{x_1}^2 &= \left(\frac{\partial x_1}{\partial \rho_1}\right)^2 \sigma_{\rho_1}^2 + \sum_i \left(\frac{\partial x_1}{\partial V_{i1}}\right)^2 \sigma_{V_{i1}}^2 \\ &+ \left(\frac{\partial x_1}{\partial \rho_2}\right)^2 \sigma_{\rho_2}^2 + \left(\frac{\partial x_1}{\partial V_2}\right)^2 \sigma_{V_2}^2 \end{aligned} \quad (E)$$

where

σ_{ρ_1} = expected error in density of component 1

σ_{V_1} = expected error in volume of component 1 injected

σ_{ρ_2} = expected error in density of component 2

σ_{V_2} = expected error in volume of component 2 injected

Expressions for the partial derivatives in Equation (E) can be derived by differentiation of Equation (D) with respect to ρ_1 , V_{i1} , ρ_2 , and V_2 which yields

$$\frac{\partial x_1}{\partial \rho_1} = \frac{\rho_2 V_2 \sum V_{i1}}{(\rho_1 \sum V_{i1} + \rho_2 V_2)^2} \quad (F)$$

$$\frac{\partial x_1}{\partial V_{i1}} = \frac{\rho_1 \rho_2 V_2}{(\rho_1 \sum V_{i1} + \rho_2 V_2)^2} \quad (G)$$

$$\frac{\partial x_1}{\partial \rho_2} = \frac{-\rho_1 V_2 \sum V_{i1}}{(\rho_1 \sum V_{i1} + \rho_2 V_2)^2} \quad (H)$$

$$\frac{\partial x_1}{\partial V_2} = \frac{-\rho_1 \rho_2 \sum V_{i1}}{(\rho_1 \sum V_{i1} + \rho_2 V_2)^2} \quad (I)$$

respectively.

After substitution of Equation (F) through (I) into Equation (E) and some algebraic manipulation, Equation (E) becomes

$$\sigma_{x_1} = x_1 x_2 \left[\left(\frac{\sigma_{\rho_1}}{\rho_1} \right)^2 + \left(\frac{\sigma_{V_1}}{\sum V_{i1}} \right)^2 + \left(\frac{\sigma_{\rho_2}}{\rho_2} \right)^2 + \left(\frac{\sigma_{V_2}}{V_2} \right)^2 \right]^{1/2}. \quad (J)$$

APPENDIX B

EXPLANATION OF THE PROGRAM USED TO CALCULATE PERCENTAGE UNCERTAINTY IN CO₂ DENSITY

This program calculated the percent uncertainty in CO₂ density as a function of pressure at a constant temperature of 50°C using the Soave-Redlich-Kwong equation of state discussed in Chapter III and the following equation developed by error propagation of the CO₂ density which is a function of both temperature and pressure:

$$\sigma_{\rho_{\text{CO}_2}} = \left[\left(\frac{\partial \rho_{\text{CO}_2}}{\partial p} \sigma_p \right)^2 + \left(\frac{\partial \rho_{\text{CO}_2}}{\partial T} \sigma_T \right)^2 \right]^{0.5}$$

where

$\sigma_{\rho_{\text{CO}_2}}$ is the uncertainty in CO₂ density

σ_p is the uncertainty in pressure

σ_T is the uncertainty in temperature

The partial derivatives and the pressure are calculated from the SRK equation of state, while the values for σ_T and σ_p , 0.1 K and 0.05 psi, respectively, are unique to the apparatus used in this study. Using these values the program generates a table showing the percent uncertainty in CO₂ density as a function of pressure.

APPENDIX C

COMPUTER PROGRAM USED TO CALCULATE CO₂ DENSITY AS A FUNCTION OF TEMPERATURE AND PRESSURE

This program calculates the density of carbon dioxide at a given temperature and pressure using an analytical equation of state developed by IUPAC. The program was set up interactively so that a density value could be calculated conveniently at the temperature and pressure conditions of a CO₂ injection. The program can handle a variety of units on the input variables which makes it very user friendly.

```

$JOB
C2345678901234567890
C
C
C      CALCULATE PRESSURE USING ANALYTICAL EQUATION OF STATE
C
C
1      IMPLICIT REAL *8 (A-G,O-Z)
2      DIMENSION BIJ(10,7),A(4),C(2),D(2)
3      DATA BIJ/-7 25854437D-01,4.47869183D-01,-1.72011999D-01,
C4 46304911D-03,2 55491571D-01,5.94667298D-02,
C-1.47960010D-01,1 36710441D-02,3 92284575D-02,
C-1 19872097D-02,-1 68332974D00,1 26050691D00,
C-1 83458178D00,-1.76300541D00,2 37414246D00,
C1.16974683D00,-1.69233071D00,-1.00492330D-01,
C4.41503812D-01,-8 46051949D-02,2.59587221D-01,
C5.96957049D00,-4 61487677D00,-1.11436705D01,
C7 50925141D00,7 43706410D00,-4.68219937D00,
C-1.63653806D00,8.86741970D-01,4 64564370D-02,
C3.76945574D-01,1.54645885D01,-3.82121926D00,
C-2.78215446D01,6.61133318D00,1.50646731D01,
C-3.13517448D00,-1 87082988D00,0 0D00,0 0D00,
C-6.70755370D-01,1 94449475D01,3 60171349D00,
C-2.71685720D01,-2 42663210D00,9 57496845D00,
C0 0D00,0.0D00,0.0D00,0.0D00,-8.71456126D-01,
C8 64880497D00,4 92265552D00,-6 42177872D00,
C-2 57944032D00,0.0D00,0.0D00,0 0D00,0.0D00,0.0D00,
C-1 49156928D-01,0 0D00,0 0D00,0 0D00,0 0D00,0 0D00,
C0 0D00,0 0D00,0 0D00,0.0D00/
4      DATA A/-6.8849249D00,-9 5924263D00,1.3679755D01,
C-8 6056439D00/
5      DATA C/3 822502D-01,4.2897885D-01/
6      WRITE(6,73)
7      73  FORMAT(/15X,'***** DETERMINATION OF CARBON DIOXIDE DENSITY *****
C*')
8      WRITE(6,74)
9      74  FORMAT(/20X,'ENTER TEMPERATURE UNITS')
10     WRITE(6,175)
11     175  FORMAT(20X,'1-FARENHEIT, 2-RANKINE, 3-KELVIN, 4-CELSIUS?')
12     READ(5,176) L1
13     176  FORMAT(I1)
14     WRITE (6,500) L1
15     500  FORMAT (20X,I1)
16     WRITE(6,177)
17     177  FORMAT(/20X,'ENTER PRESSURE UNITS')
18     WRITE(6,178)
19     178  FORMAT(20X,'1-PSIA, 2-ATM, 3-BAR ?')
20     READ(5,79) L2
21     79  FORMAT(I1)
22     WRITE (6,502) L2
23     502  FORMAT (20X,I1)
24     WRITE(6,81)
25     81  FORMAT(/20X,'ENTER DESIRED DENSITY UNITS')
26     WRITE(6,82)
27     82  FORMAT(20X,'1-G/CM3, 2-LB/FT3 ?')
28     READ(5,83) L3
29     83  FORMAT(I1)
30     WRITE (6,503) L3
31     503  FORMAT (20X,I1)

```

```

00000080
00000090
00000100
00000110
00000120
00000130
00000140
00000150
00000160
00000170
00000180
00000190
00000200
00000210
00000220
00000230
00000240
00000250
00000260
00000270
00000280
00000290
00000300
00000310
00000320
00000330
00000340
00000350
00000360
00000370
00000380
00000390
00000400
00000410
00000420
00000430
00000440
00000450
00000460
00000470
00000480
00000490
00000500
00000510
00000520
00000530
00000540
00000550
00000560
00000570
00000580
00000590
00000600
00000610
00000620
00000630
00000640
00000650
00000651
00000652

```



```

32      WRITE(6,199)
33 199  FORMAT(/5X,'FIX DECIMAL POINT WHEN ENTERING ALL REQUESTED DATA
      C'//)
34      WRITE(6,84)
35 84   FORMAT(/5X,'ENTER INITIAL TEMPERATURE')
36      READ(5,86) T
37 86   FORMAT(D10 4)
38      WRITE (6,504) T
39 504  FORMAT (5X,F7 2)
40      WRITE(6,87)
41 87   FORMAT(/5X,'ENTER FINAL TEMPERATURE')
42      READ(5,88) TFIN
43 88   FORMAT(D10 4)
44      WRITE (6,505) TFIN
45 505  FORMAT (5X,F7 2)
46      WRITE(6,89)
47 89   FORMAT(/5X,'ENTER TEMPERATURE INCREMENT')
48      READ(5,91)TINC
49 91   FORMAT(D10 4)
50      WRITE (6,506) TINC
51 506  FORMAT (5X,F7 2)
52      WRITE(6,92)
53 92   FORMAT(/5X,'ENTER INITIAL PRESSURE')
54      READ(5,93)P
55 93   FORMAT(D10 4)
56      WRITE (6,507) P
57 507  FORMAT (5X,F7 2)
58      WRITE(6,94)
59 94   FORMAT(/5X,'ENTER FINAL PRESSURE')
60      READ(5,95) PFIN
61      WRITE (6,508) PFIN
62 508  FORMAT (5X,F7 2)
63 95   FORMAT(D10 4)
64      WRITE(6,96)
65 96   FORMAT(/5X,'ENTER PRESSURE INCREMENT')
66      READ(5,97)PINC
67 97   FORMAT(D10 4)
68      WRITE (6,509) PINC
69 509  FORMAT (5X,F7 2)
70      WRITE(6,135)
71 135  FORMAT(/5X,'OUTPUT UNITS ARE ')
72      IF(L1 EQ 1)GO TO 251
73      IF(L1 EQ 2)GO TO 252
74      IF(L1 EQ 4)GO TO 253
75      IF(L1 EQ 3)GO TO 302
76 251  T=(T+460)/1 8
77      TFIN=(TFIN+460 0)/1 8
78      TINC=TINC/1 8
79      WRITE(6,136)
80 136  FORMAT(5X,'TEMPERATURE - DEGREES FARENHEIT')
81      GO TO 254
82 252  T=T/1 8
83      TFIN=TFIN/1 8
84      TINC=TINC/1 8
85      WRITE(6,137)
86 137  FORMAT(5X,'TEMPERATURE - DEGREES RANKINE')
87      GO TO 254
88 253  T=T+273. 15
89      TFIN=TFIN+273 15
90      WRITE(6,138)

```

```

00000660
00000670
00000680
00000690
00000700
00000710
00000720
00000721
00000722
00000730
00000740
00000750
00000760
00000761
00000762
00000770
00000780
00000790
00000800
00000801
00000802
00000810
00000820
00000830
00000840
00000841
00000842
00000850
00000860
00000870
00000871
00000872
00000880
00000890
00000900
00000910
00000920
00000921
00000922
00000930
00000940
00000950
00000960
00000970
00000980
00000990
00001000
00001010
00001020
00001030
00001040
00001050
00001060
00001070
00001080
00001090
00001100
00001110
00001120
00001130

```

```

91 138 FORMAT(5X,'TEMPERATURE - DEGREES CELSIUS') 00001140
92 GO TO 254 00001150
93 302 WRITE(6,303) 00001160
94 303 FORMAT(5X,'TEMPERATURE - DEGREES KELVIN') 00001170
95 254 IF(L2 EQ 1)GO TO 155 00001180
96 IF(L2 EQ 2)GO TO 156 00001190
97 IF(L2 EQ 3)GO TO 305 00001200
98 155 P=0 068947*P 00001210
99 PINC=0 068947*PINC 00001220
100 PFIN=0 068947*PFIN 00001230
101 WRITE(6,141) 00001240
102 141 FORMAT(5X,'PRESSURE - PSIA') 00001250
103 GO TO 257 00001260
104 156 P=1 01325*P 00001270
105 PINC=1 01325*PINC 00001280
106 PFIN=1 01325*PFIN 00001290
107 WRITE(6,142) 00001300
108 142 FORMAT(5X,'PRESSURE - ATMOSPHERES') 00001310
109 GO TO 257 00001320
110 305 WRITE(6,306) 00001330
111 306 FORMAT(5X,'PRESSURE - BAR') 00001340
112 257 IF (L3 EQ 1)GO TO 310 00001350
113 WRITE(6,311) 00001360
114 311 FORMAT(5X,'DENSITY - POUNDS PER CUBIC FT') 00001370
115 GO TO 340 00001380
116 310 WRITE(6,312) 00001390
117 312 FORMAT(5X,'DENSITY - GRAMS PER CM3') 00001400
118 340 WRITE(6,98) 00001410
119 98 FORMAT(//10X 'PRESSURE',8X,'TEMPERATURE',8X,'CO2 DENSITY',13X,'Z')00001420
120 WRITE(6,99) 00001430
121 99 FORMAT(9X,'-----',6X,'-----',6X, 00001440
C'-----',7X,'-----'/) 00001450
122 401 PIN=P 00001460
123 402 P=PIN 00001470
124 78 TC=304 21 00001480
125 PC=73 825 00001490
126 RHOC=0 010589 00001500
127 R=83 143 00001510
128 IF(T GT TC)GO TO 22 00001520
129 PSUM=0 0 00001530
130 DO 23 I=1,4 00001540
131 PCONST=A(I)*(1C/T-1)**I 00001550
132 PSUM=PSUM+PCONST 00001560
133 23 CONTINUE 00001570
134 PSAI=PC*DEXP(11 3774*(1-T/1C)**1 935+PSUM) 00001580
135 IF(P LT PSAI)GO TO 22 00001590
136 SUM=0 0 00001600
137 DO 26 I=1,2 00001610
138 CON=C(I)*(1-T/1C)**((I+1 0)/3 0) 00001620
139 SUM=SUM+CON 00001630
140 26 CONTINUE 00001640
141 RHO=RHOC*(1+1 9073793*(1 T/1C)**0 347+SUM) 00001650
142 28 GO TO 41 00001660
143 22 RHO=P/(R*T) 00001670
144 41 M=0 00001680
145 31 SUM=0 0 00001690
146 TAU=304 2/T 00001700
147 OMEGA=RHO/O 01063 00001710
148 DO 100 J=1,7 00001720
149 DO 90 I=1,10 00001730

```

```

150          CONST=BIJ(I,J)*(IAU-1)**(J-1)*(OMEGA-1)**(I-1)      00001740
151          SUM=SUM+CONST      00001750
152          90 CONTINUE      00001760
153          100 CONTINUE      00001770
154          Z=1.0+OMEGA*SUM      00001780
155          R=83.143      00001790
156          PA=RHO*Z*R*T      00001800
C      00001810
C      00001820
C      00001830
C      00001840
C      CALCULATE CRITICAL EQUATION PARAMETERS      00001850
C      00001860
C      00001870
157          DELT=DABS((I-TC)/TC)      00001880
158          DELRHO=DABS((RHO-RHOC)/RHOC)      00001890
159          R=DELT*(0.6471102*DELRHO**2)**1.4409      00001900
160          25 X=R-0.6471102*R**0.306*DELRHO**2-DELT      00001910
161          ABSX=DABS(X)      00001920
162          IF (ABSX LT 1E-5)GO TO 20      00001930
163          DX=1-0.198016*DELRHO**2/R**0.694      00001940
164          R=R-X/DX      00001950
165          GO TO 25      00001960
166          20 THETA=0.670302*DELRHO/R**0.347      00001970
167          QT1=37.26895-82.70074*THETA**2+57.08947*THETA**4.0      00001980
168          IF (T GE TC)GO TO 30      00001990
169          CCAL=-53.81157      00002000
170          GO TO 40      00002010
171          30 CCAL=-34.92493      00002020
172          40 QT2=CCAL*DABS(1.0-1.440248*THETA**2.0)**1.934872      00002030
173          QTHETA=QT1+QT2      00002040
174          DELP=R**1.9348*QTHETA+6.98*DELT+28.362      00002050
C          *R**1.5879*THETA*(1-THETA**2)      00002060
175          PS=PC*(1+DELP)      00002070
C      00002080
C      THE FINAL EQUATION      00002090
C      00002100
176          EXP1=1-DEXP(-(0.01/R)**1.5)      00002110
177          EXP2=1-DEXP(-(0.05/R)**3.0)      00002120
178          FR=1-EXP1*EXP2      00002130
179          PCALC=FR*PA+(1-FR)*PS      00002140
180          LRR=DABS(P-PCALC)/P      00002150
181          IF (LRR LT 1E-4)GO TO 160      00002160
182          IF (M EQ 0)GO TO 131      00002170
183          DRHODP=(RHODEL-RHOOLD)/(PCALC-POLD)      00002180
184          RHO=RHOOLD+DRHODP*(P-POLD)      00002190
185          GO TO 41      00002200
186          131 M=1      00002210
187          POLD=PCALC      00002220
188          RHOOLD=RHO      00002230
189          DEL=0.001      00002240
190          RHODEL=RHO+DEL      00002250
191          RHO=RHODEL      00002260
192          GO TO 31      00002270
193          160 RHO=RHO*44.009      00002280
194          IF (L1 EQ 1)GO TO 350      00002290
195          IF (L1 EQ 2)GO TO 351      00002300
196          IF (L1 EQ 4)GO TO 352      00002310
197          GO TO 353      00002320
198          350 HIT=1.8*T-460      00002330

```

```

199      GO TO 453                                00002340
200 351 HT4-1 8*1                                00002350
201      GO TO 453                                00002360
202 352 HT4-1-273 15                            00002370
203      GO TO 453                                00002380
204 353 HT4-1                                    00002390
205 453 IF (L2 EQ 1)GO TO 354                    00002400
206      IF (L2 EQ 2)GO TO 255                    00002410
207      GO TO 356                                  00002420
208 354 HP4-14 504*P                              00002430
209      GO TO 256                                  00002440
210 255 HP4=P/1.01325                              00002450
211      GO TO 256                                  00002460
212 356 HP4-P                                      00002470
213 256 IF (L3 EQ 1)GO TO 378                    00002480
214      HRH01=RHO*62 371                          00002490
215      GO TO 379                                  00002500
216 378 HRH01=RHO                                  00002510
217 379 R=83 143                                   00002520
218      Z=(P/ALC*44 009)/(RHO*R*T)                00002530
219      HZ=Z                                        00002540
220      WRITE (6,170)HP4,HT4,HRH04,HZ            00002550
221 170 FORMAT(7X,F10 2,8X,F10 2 10X,1 TO 6,8X,F10 5) 00002560
222      P=PFINC                                    00002570
223      IF (PINC EQ 0 0)GO TO 75                  00002580
224      IF (P GT PFIN)GO TO 75                    00002590
225      GO TO 78                                    00002600
226 75 P=P+PINC                                    00002610
227      IF (PINC EQ 0 0)GO TO 77                  00002620
228      IF (P GT PFIN)GO TO 77                    00002630
229      GO TO 402                                   00002640
230 77 STOP                                        00002650
231      END                                        00002660

$ENTRY                                           00002670

```

***** DETERMINATION OF CARBON DIOXIDE DENSITY *****

ENTER TEMPERATURE UNITS
1-FARENHEIT, 2-RANKINE, 3-KELVIN, 4-CELSIUS?
1

ENTER PRESSURE UNITS
1-PSIA, 2-ATM, 3-BAR ?
1

ENTER DESIRED DENSITY UNITS
1-G/CM³, 2-LB/FT³ ?
1

FIX DECIMAL POINT WHEN ENTERING ALL REQUESTED DATA

ENTER INITIAL TEMPERATURE
212 00

ENTER FINAL TEMPERATURE
212 00

ENTER TEMPERATURE INCREMENT
0.00

ENTER INITIAL PRESSURE
700 00

ENTER FINAL PRESSURE
730 00

ENTER PRESSURE INCREMENT
10 00

OUTPUT UNITS ARE
TEMPERATURE - DEGREES FARENHEIT
PRESSURE - PSIA
DENSITY - GRAMS PER CM3

----- PRESSURE -----	----- TEMPERATURE -----	----- CO2 DENSITY -----	----- Z -----
700 01	212 00	0 077497	0 88298
710 01	212 00	0.078758	0 88125
720 01	212 00	0 080024	0 87953
730 01	212 00	0.081295	0.87780

STATEMENTS EXECUTED= 512

CORE USAGE OBJECT CODE= 9936 BYTES, ARRAY AREA= 624 BYTES, TOTAL AREA AVAILABLE= 129024 BYTES

DIAGNOSTICS NUMBER OF ERRORS= 0, NUMBER OF WARNINGS= 0, NUMBER OF EXTENSIONS= 0

COMPILE TIME= 0 09 SEC, EXECUTION TIME= 0 07 SEC, 11 02 39 THURSDAY 4 OCT 84 WATFIV - MAR 1980 V2LO

C\$STOP

APPENDIX D

COMPUTER PROGRAM USED TO CALIBRATE PRESSURE TRANSDUCERS

This is an iterative program which calculates the hydrocarbon transducer correction used to adjust experimental pressure measurements taken with the bubble point apparatus. The gauge correction is calculated as the difference between the actual transducer pressure readout and the Ruska dead weight gauge reference pressure. The Ruska pressure is calculated from an equation supplied in the manual which accompanied the dead weight gauge tester. The equation (shown in lines 24-28 of the program) is a function of several variables; the sum of the masses placed on the floating piston (SUMMAS (M)), the tare mass of the floating piston (TARMAS), acceleration due to gravity (C1), the temperature of the floating piston hydraulic oil (TEMP), the transducer pressure reading (GAUGE (N,M)), and five constants (C2-C6) which are supplied by the manual. After the reference pressure is calculated, the head correction is subtracted from it to account for the difference in fluid levels between the mercury in the equilibrium cell and the dead weight gauge tester reference line. The head correction is calculated as follows:

$$HC = g[\rho_{Hg}(h_{Hgcell} - h_{interface}) - \rho_{oil}(h_{ref} - h_{interface})]$$

where

HC is the head correction
 g is the acceleration due to gravity
 ρ_{Hg} is the density of mercury (at 50°C)
 h_{Hgcell} is the height of the mercury in the equilibrium cell
 $h_{interface}$ is the height of the mercury-oil interface
 ρ_{oil} is the density of the dead weight gauge tester hydraulic oil
 h_{ref} is the height of the dead weight gauge tester reference line

After substituting the values of the various heights measured with the cathetometer, $h_{Hgcell} = 577.5\text{mm}$, $h_{interface} = 116.95\text{mm}$, and $h_{ref} = 223.3\text{mm}$, as well as an appropriate value for the acceleration due to gravity, a value for HC is calculated from the equation to be 8.7 psi. Once the values for the head correction and the various transducer gauge pressure readings have been read into the program, a table is printed out which can be used to determine the correct gauge correction required at any pressure within the set range of calibration. A useful list of weight combinations (Table D) is included to show the combinations of weights used and the corresponding dead weight reference pressures calculated using those combinations.

```

$JOB                                00000061
C                                    00000070
C                                    00000080
C      THIS PROGRAM CALCULATES TRANSDUCER CORRECTIONS FOR THE PRESSURE 00000090
C      HYDROCARBON TRANSDUCER LOCATED IN EN412 FROM DEAD WEIGHT        00000100
C      TEST DATA                                                       00000110
C                                    00000120
C                                    00000130
C      USER I D U14702F                                                00000140
C      PROGRAM NAME 1CPRSS CNFL                                         00000150
C                                    00000160
C                                    00000170
C                                    00000180
1      DIMENSION SUMMAS(21),GAUGE(2,21),DWP(2,21),GC(2,21),          00000190
      TRANSP(2,21),HEAD(2),GAUGE(2)                                     00000200
2      DOUBLE PRECISION C1,C2                                           00000210
3      DATA C1,C2,C3,C4/O 998951759.0 0260416.1 0.0 000017/         00000220
4      DATA C5,C6/25 0.0 2356E-08/                                     00000230
5      DATA TEMP/24 4/                                                00000240
6      DATA HEAD/B 7.0 O/                                              00000250
7      DATA NUMP,TARMAS/21.0 78107/                                    00000260
8      DATA MONTH,NDATE,NYEAR/8.28.84/                                00000270
9      DO 20 N=1,2                                                       00000280
10     DO 10 M=1,NUMP                                                    00000290
11     READ (5,5) TRANSP(N,M)                                           00000300
12     5   FORMAT (F9.3)                                                00000310
13     10  CONTINUE                                                     00000320
14     20  CONTINUE                                                     00000330
15     DO 40 N=1,2                                                       00000340
16     DO 30 M=1,NUMP                                                    00000350
17     GAUGE(N,M) = TRANSP(N,M) - 14 696                                00000360
18     30  CONTINUE                                                     00000370
19     40  CONTINUE                                                     00000380
20     READ (5,50) (SUMMAS(I),I=1,NUMP)                                  00000390
21     50  FORMAT (F10.6)                                               00000400
22     DO 70 N=1,2                                                       00000410
23     DO 60 M=1,NUMP                                                    00000420
24     DWP(N,M) = (SUMMAS(M) + TARMAS)*C1                               00000430
25     DWP(N,M) = C2*(C3 + C4*(TEMP - C5))*(C3 - C6*GAUGE(N,M))       00000440
26     DWP(N,M) = DWP(N,M)/DWP(N,M)                                    00000450
27     TRUEP = DWP(N,M) - HEAD(N)                                       00000460
28     GC(N,M) = TRUEP - GAUGE(N,M)                                     00000470
29     60  CONTINUE                                                     00000480
30     70  CONTINUE                                                     00000490
31     WRITE (6,120) MONTH,NDATE,NYEAR                                  00000491
32     120 FORMAT (///40X,'DATE',1X,I2,'/',1X,I2,'/',1X,I2,/)          00000501
33     WRITE (6,130)                                                     00000511
34     130 FORMAT (10X,'INPUT UNITS ARE DEG C AND PSIA'////)          00000521
35     WRITE (6,80)                                                      00000522
36     80  FORMAT (///20X 'HYDROCARBON TRANSDUCER CORRECTIONS'///)    00000523
37     WRITE (6,90)                                                      00000524
38     90  FORMAT (15X,'TRANS PRESS',5X,'D W PRESS',5X,'TRANSD CORR'//) 00000530
39     WRITE (6,100) (TRANSP(1,M),DWP(1,M),GC(1,M),M=1,NUMP)          00000540
40     100 FORMAT (18X,F7.2,8X,F7.2,9X,F5.2)                            00000550
41     WRITE (6,110)                                                     00000560
42     110 FORMAT (/1X,'-----'//,1X,'-----'//,1X,'-----'//) 00000561
C 110 FORMAT (///25X,'GAS TRANSDUCER CORRECTIONS'///)                 00000562
C     WRITE (6,90)                                                      00000570
C     WRITE (6,100) (TRANSP(2,M),DWP(2,M),GC(2,M),M=1,NUMP)          00000580

```


43 STOP
44 END

00000640
00000650

\$ENTRY

00000660

DATE. 8/28/84

INPUT UNITS ARE DEG C AND PSIA

HYDROCARBON TRANSDUCER CORRECTIONS

TRANS PRESS	D W PRESS	TRANSD CORR
57 90	49 94	-1 97
87 60	79.90	-1 70
137 30	129 84	-1 47
186 90	179 77	-1 13
236 50	229 71	-0 79
256 30	249 68	-0 62
286 10	279 65	-0 46
385 30	379 52	0 22
435 00	429 46	0 45
534 10	529 33	1 23
633 40	629 21	1 80
732 50	729 08	2 58
831 70	829 03	3 33
930 90	928 83	3 93
1030 00	1028 70	4 70
1129 20	1128 58	5 38
1228 30	1228 42	6 12
1327 40	1328 30	6 90
1426 50	1428 17	7 67
1525 60	1528 05	8 44
1624 60	1627 93	9 32

STATEMENTS EXECUTED= 442

CORE USAGE OBJECT CODE= 2672 BYTES,ARRAY AREA= 772 BYTES,TOTAL AREA AVAILABLE= 129024 BYTES

TABLE D

Weight Combination	Resulting Reference Pressure, psig
Q	49.94
P	79.90
O	129.84
O, P	179.77
M	229.71
M, Q	249.68
M, P	279.65
N, O, P	379.52
M, N	429.08
M, N, O	529.33
L, O	629.21
L, M	729.08
L, M, O	829.03
L, M, N	928.83
L, M, N, O	1028.70
A, O	1128.58
A, N	1228.42
A, M, O	1328.30
A, M, N	1428.17
A, M, N, O	1528.05
A, L, O	1627.93

APPENDIX E

EXPLANATION OF TABLE VI

Table VI may be used to recalculate solubilities in the event that discrepancies are found between values for the solvent or CO₂ densities used in this study and values from other literature sources or experimental works. To convert the solubilities used in this study to values which correspond to densities from other sources, the following guidelines may be used:

Case 1: New Solvent Densities

If the CO₂ densities agree with the preferred source but the solvent density needs to be changed;

- a. Divide column 2 of Table VI by column 1, then multiply the resulting value by the preferred solvent density. The value calculated will be the gram moles of solvent injected, consistent with the new density used.
- b. Repeat step (a) for each solvent injection (see column 6)
- c. Using Equation A (Appendix A), recalculate new solubilities remembering to use the values in column 5 of Table VI for n_1 and the value calculated in step (a) for n_2 .

Case 2: New CO₂ Densities

If only the CO₂ densities are in disagreement with the preferred source:

- a. Divide column 5 of Table VI by column 4 and multiply the resulting value by the preferred CO₂ density. This calculation will produce a value for the gram moles of CO₂ injected consistent with the desired CO₂ density.
- b. Repeat step (a) for each row where the CO₂ densities do not agree.
- c. Recalculate solubilities using Equation (A) (Appendix A) remembering to use the newly calculated values for n_1 while keeping the same values for n_2 as found in column 2 of Table VI.

Case 3: New Solvent and CO₂ Densities

If both densities disagree, then combine the steps in the previous conditions to recalculate the preferred solubilities.

VITA 2

John McRay Anderson

Candidate for the Degree of
Master Of Science

Thesis: HIGH PRESSURE SOLUBILITIES OF CARBON DIOXIDE IN BENZENE,
CYCLOHEXANE, NAPHTHALENE, AND TRANS-DECALIN

Major Field: Chemical Engineering

Biographical:

Personal Data: Born in Wynnewood, Oklahoma, October 10, 1960, the son of John Morton and Ruth Alice Anderson. Other family members include a younger brother, Bryan Edward, a younger sister, Tammie Ruth, and an older sister, Jackie Lynn Whitely and her husband, Collin Whitley. Presently single and employed by Texas Instruments.

Education: Attended Sulphur High School in Sulphur, Oklahoma; graduated Valedictorian in 1979; received the Bachelor of Science degree in Chemical Engineering from the Oklahoma State University in July, 1983; completed the requirements for the Master of Science degree in May, 1985.